Author/s:
Li, J;Shepelin, NA;Sherrell, PC;Ellis, AV

Title:
Poly(dimethylsiloxane) for Triboelectricity: From Mechanisms to Practical Strategies

Date:
2021-06-22

Citation:
Li, J., Shepelin, N. A., Sherrell, P. C. & Ellis, A. V. (2021). Poly(dimethylsiloxane) for Triboelectricity: From Mechanisms to Practical Strategies. Chemistry of Materials, 33 (12), pp.4304-4327. https://doi.org/10.1021/acs.chemmater.1c01275.

Persistent Link:
https://hdl.handle.net/11343/275072

Poly(dimethylsiloxane) for Triboelectricity – From Mechanisms to Practical Strategies

Jingyi Li,[1] Nick A. Shepelin,[1,2] Peter C. Sherrell,[1*] and Amanda V. Ellis[1*]

[1] Department of Chemical Engineering, The University of Melbourne, Parkville, Victoria, 3010, Australia

[2] Laboratory for Multiscale Materials Experiments, Paul Scherrer Institut, CH-5232 Villigen PSI, Switzerland

*Prof. Amanda V. Ellis: amanda.ellis@unimelb.edu.au ; Dr Peter C. Sherrell: peter.sherrell@unimelb.edu.au

ABSTRACT: The triboelectric effect (TE), simply described as the generation of electricity from tribology or friction, has been known for over 1500 years. TE arises from charge transfer between surfaces under contact, typically attributed to electron transfer. However, emerging understanding shows how the ion transfer and material transfer (bond cleavage) mechanisms play a key role in TE. An engineering focus on increasing the porosity, surface roughness, and use of heterogenous materials has resulted in a recent explosion in triboelectric literature, particularly towards soft and flexible polymer devices. Here, we critically evaluate recent progress in TE generators and link engineered performance to the fundamental driving forces of triboelectricity, using the exemplar triboelectric polymer, poly(dimethylsiloxane).

1. Introduction

The triboelectric effect, which generates electrical charge from tribology, occurs when two electrically neutral materials are bought in contact. The relative motion causes surface charges to be transferred between the two materials, and the subsequent separation of the materials results in an opposing surface electrical charge.[1] The triboelectric effect occurs among a diverse range of materials, including polymers, metals, and ceramics. Consequently, as a result of rigorous empirical studies, the extent of the charge between pairs of materials, as well as the directionality (i.e., positively and negatively charged constituents), has culminated in the triboelectric series.[2]

The triboelectric series (Figure 1) provides a list of materials in order of the likelihood of possessing positive or negative surface charge following a contact-separation interaction. It provides a guide to both the 'sign' and magnitude of the charge generated from a contact separation interaction, dependent upon the relative position, and degree of separation of the two materials. However, since the series is empirically obtained, many different, and indeed contradictory, triboelectric series have been published.[2]

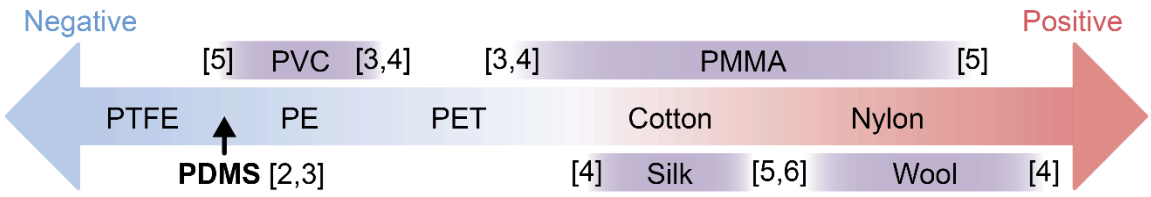

Figure 1. Illustration of the triboelectric series, highlighting the relative position of poly(dimethylsiloxane) (PDMS)[2, 3] at a negative position, and showing the large variations in positions of wool, silk, poly(methyl methacrylate) (PMMA), and poly(vinyl chloride) (PVC) in literature.[1, 4-7]

These contradictory triboelectric series clearly highlight that the mechanisms driving triboelectric charging are poorly understood, and that the generated charge cannot be understood by simple differences in chemical composition. It is apparent that the order of the triboelectric series is not only influenced by intrinsic material properties, but also incorporates effects from other factors, including the texture of the material,[8] applied force/pressure,[9] and environmental conditions (e.g., humidity, pressure[10] and temperature[11]). Here, the complexity of triboelectricity becomes apparent, and it is important to clarify the difference between contact electrification (CE) and triboelectrification (TE).

CE and TE are often used interchangeably in literature, as both phenomena represent the electrification process under relative motion between two materials. However, to a deeper extent, the exact motion of the contacting layers differs between the CE and TE mechanisms.[12] The CE mechanism occurs solely under vertical physical contact—without horizontal friction—offering better control and thus leading to a well-defined understanding. Conversely, the TE mechanism involves both frictional and compressive components, resulting in an increasingly general phenomenon.[12] Relative to CE, the TE process is significantly more complicated and incorporates extra degrees of motion (e.g., shearing or sliding), which influences the charge transfer and separation processes. Therefore, while CE and TE are closely related, hypotheses derived from the study of CE cannot fully describe the ongoing processes in TE.

In this review, the discussion of the CE mechanism will focus on fundamental studies of molecular scale processes, while the discussion of the TE mechanism will focus on the studies involving experiments at the macroscopic scale. When referring to the general concept of charging by contact/friction, CE will be used.

With a combination of strong triboelectric surface charging and tunable mechanical properties, poly(dimethylsiloxane) (PDMS) is an ideal choice for making triboelectric generator (TEG) devices and probing the fundamental mechanisms of CE, in order to provide a key connection between theoretical foundations and practical devices. PDMS is also considered a strongly negative triboelectric material, [2, 3] meaning it typically accumulates a strong negative surface charge following mechanical contact with other materials.

Thus, this review will discuss the complexity of triboelectric energy generation, using PDMS as a case study due

to its ubiquity in literature. The current understandings and ambiguities surrounding the fundamental mechanisms governing the triboelectric effect will be critically reviewed, along with the influences of both the materials chemistry and surface engineering on the resultant TEG device performance. Critically, the results observed in experimental studies on PDMS-based triboelectric materials will be meticulously correlated to the fundamental mechanisms and engineering approaches.

2. Poly(dimethylsiloxane) – an ideal triboelectric material

PDMS is a polymer that consists of an inorganic backbone with alternating silicon (Si) and oxygen (O) atoms with two methyl groups attached to the Si (Figure 2, (a)). The Pauling electronegativity difference between Si and O is 1.7, exhibiting a high dissociation energy of 445 kJ/mol,[13] which results in excellent thermal and chemical stability of the PDMS. The bond angle of the backbone Si-O-Si bonds is 143°, which imparts mechanical flexibility to the bulk PDMS, whilst permitting easy rearrangement of the backbone, allowing the methyl groups to be placed at the surface and interfaces.[14] Moreover, PDMS possesses a low surface free energy, defined by the molar mass and closely bonded methyl groups, imparting hydrophobic properties to the polymer.[15] The ionic nature of the Si-O and Si-C bonds unlock the possibility for the fragmentation of PDMS into radicals.[16, 17] In general, PDMS is an elastic and hydrophobic material with low dielectric constant and can be easily produced with low cost. The ability to fragment is attractive as it can promote CE, while mechanical flexibility provides more effective mechanical motion harvesting. Thus, PDMS has been a highly attractive material for TEGs.

The bulk properties of PDMS (e.g., mechanical elasticity, visible light transparency and energy harvesting) can be tailored by the variation of the two-pot (base and curing agent) mixture ratios, the reaction conditions and/or the inclusion of fillers or other molecules. For example, the mixing ratio between the base and the curing agent is typically exploited to tune the stiffness of PDMS (Figure 2(b)).[18, 19] Pristine PDMS films are typically fabricated by either spin-coating, or by pouring directly onto a substrate or into a mold prior to the curing process. Aside from bulk modification, structural modification can further tune the properties of PDMS, for example the hydrophobicity of the PDMS films can be tailored by altering the surface morphology. The examples of structurally modifying PDMS include; (1) replica molding, whereby PDMS is cast into a mold with the desired surface structure and cured (Figure 2(c));[8, 20-23] (2) direct printing of uncured PDMS with the desired pattern, followed by curing (Figure 2(d));[24] and (3) direct writing of patterns on a cured PDMS film (Figure 2(e)).[19] In-depth analyses on the modification strategies to tailor PDMS surface and bulk properties, and to fabricate sponge-like PDMS films, are presented in the reviews by Wolf *et al.*[25] and Zhu *et al.*,[26] respectively.

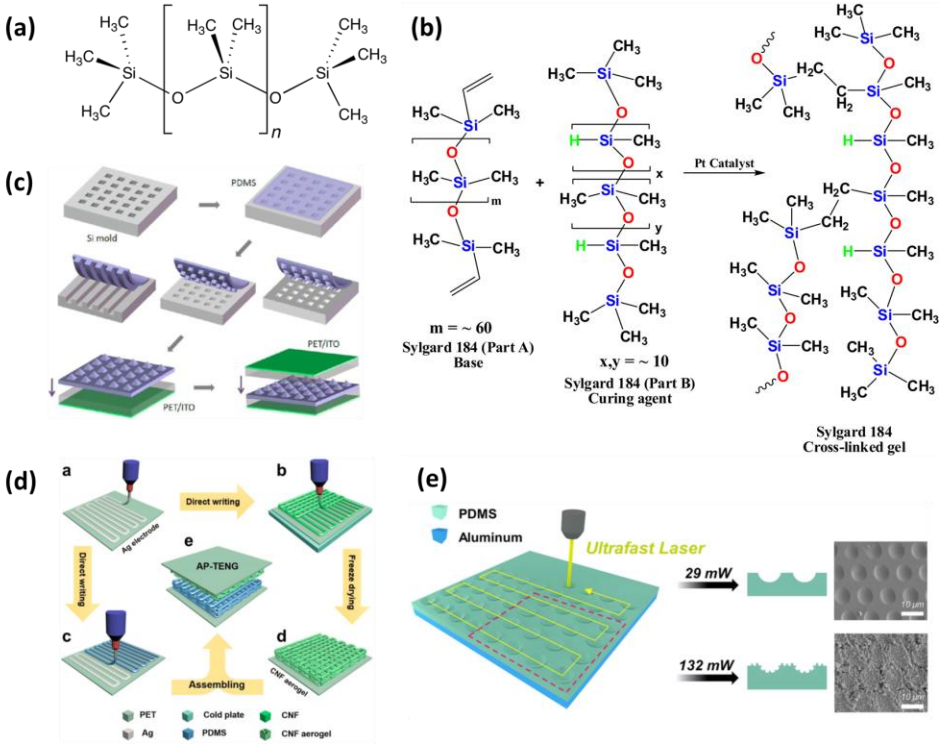

Figure 2. Synthesis of crosslinked PDMS and surface patterning methods of PDMS films. (a) The chemical formula of PDMS. (b) Reaction pathway for the synthesis of crosslinked PDMS. Reproduced with permission.[27] Copyright 2018, Elsevier. (c) Replica molding of PDMS. Reprinted with permission.[8] Copyright 2012, American Chemical Society. (d) Direct printing of structures using PDMS precursors. Reproduced with permission.[24] Copyright 2019, Elsevier. (e) Laser writing of patterns on a crosslinked PDMS film. Reproduced with permission.[19] Copyright 2017, Elsevier.

3. Fundamentals of Triboelectric Energy Generators (TEGs)

3.1. Understanding Performance

As two triboelectric layers are brought into contact under an external mechanical stress (i.e., applied force), the distance between the two layers reduces, while the effective contact area increases. Charges can be transferred between the two layers during this process. When the two layers are in the separation regime where charges can occur, the layers are considered in real contact.[28] When the stress is removed and the layers start to separate, the movement of separated charges arising from TE coupling leads to an electrostatic induction effect, consequently generating a potential difference between the two electrodes attached on the backside of the triboelectric layers (Figure 3). Under short-circuit conditions (i.e., load resistance significantly lower than the input impedance of the TEG), the potential difference induced by TE drives electrons to flow between the two electrodes via the external load, quantified by the short circuit current (I_{sc}), which can be utilized for TEG applications. Under open-circuit conditions, an open-circuit voltage (V_{oc}) can be detected, representing the degree of TE.

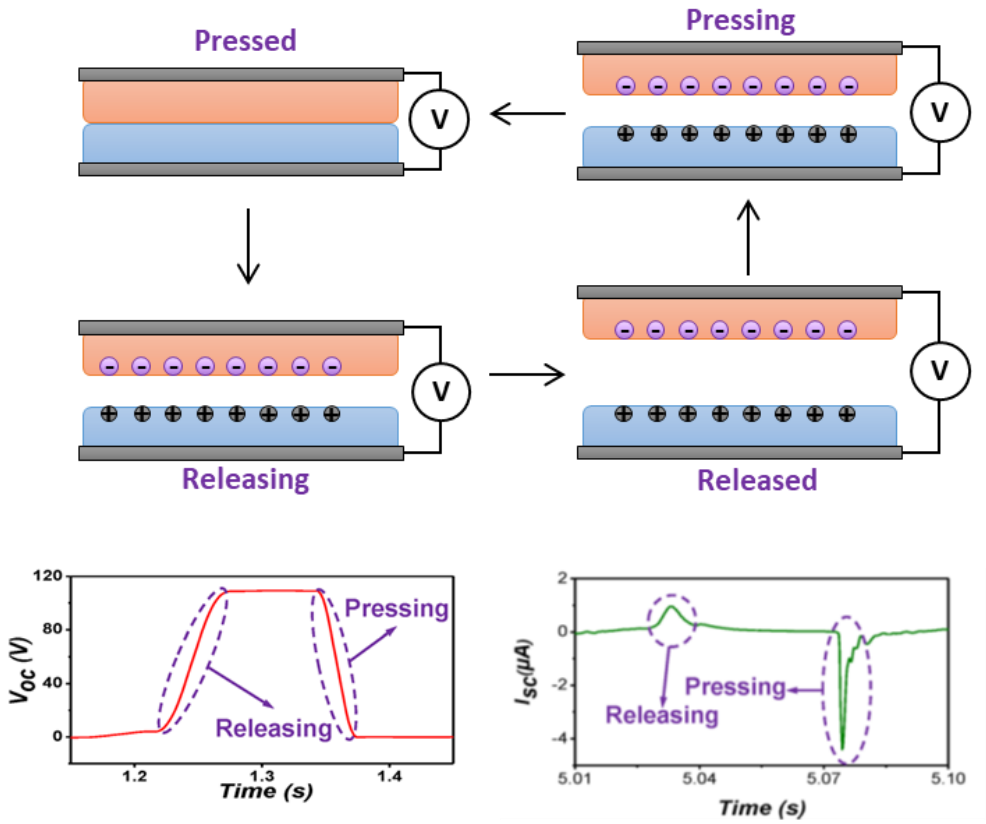

Figure 3. Diagram of the basic operational principle for the contact-separation TEG, and the corresponding open circuit voltage (V_{oc}) and short circuit current (I_{sc}) signals during each stage of compression.[8] Reprinted with permission from, [8] Copyright 2012, American Chemical Society.

Fundamentally, the degree of TE is represented by the surface charge density after contact, while the electric performance of a TEG is often represented by its peak value of under contact-separation motion with a specific contact force, frequency and load resistance. Both the V_{oc} and the I_{sc} are a direct result of the generation of surface charge due to TE, and decrease as the distance between two layers increases in the separation process.[29]

3.2. Performance for Energy Generation in poly(dimethylsiloxane)

In a traditional TEG device configuration, PDMS is typically used as the negative triboelectric layer, while the positive triboelectric layer is often comprised of metals (e.g., Al,[8, 19-23] Cu[19] or Au[30]) or polymers (e.g., poly(ethylene terephthalate) (PET)[8] or poly(methyl methacrylate) (PMMA)[31]). The interaction between the two surfaces varies dramatically depending on the choice of material for the positive layer, leading to significant variations in performance. The performance of any two pairs of triboelectric materials can be enhanced through chemical and physical modification, either on the bulk scale or through surface modification. The most commonly reported physical modification strategies are the tailoring of material properties by coating/functionalizing the contact surface[32] and/or introducing fillers into the PDMS matrix, such as inorganic particles,[33] metal organic frameworks (MOFs),[34] liquid solutions,[35] and other electronegative polymers.[36, 37] Another straightforward strategy is to modify the surface structure of the layers.[32] An in-depth analysis of materials used for TEGs and specific materials

designed to improve electrical output is presented by Kim *et al.*,[38] and a comprehensive review on strategies for controlling the surface charge generated by CE is provided by Chen *et al.*[32] Generally, modification strategies intend to enhance output performance through the following two methods; (1) physical structure modification, with the primary aim of increasing the real contact area; and (2) chemical and compositional modification, with the primary aim of increasing the disparity in electrical polarity between the two layers. In the following section, we will build on these reports, incorporating a link between the fundamental theories of charge transfer in CE and the experimental TE results.

3.3. Poly(dimethylsiloxane) modification

The compositional modification of PDMS is a powerful and often overlooked method for tailoring the triboelectric characteristics. The chemical halogenation of PDMS has been demonstrated to enhance the TE effects, owing to the strong electron affinity of the introduced halogens. For instance, Song *et al.*[39] have assembled fluorine terminated monolayers on the surface of PDMS, significantly enhancing the electrical output (from 17.3 V to 105 V) under relatively gentle mechanical contact.

Similarly, halide-based additives (e.g., fluoroethylene carbonate and benzyl chloride) have been observed to alter the electronic structure of the surrounding PDMS matrix and increase the triboelectric performance.[35] Feng *et al.*[40] have added barium titanate ($BaTiO_3$) nanoparticles and multiwalled carbon nanotubes (MWCNTs) into a PDMS matrix to form a nanocomposite triboelectric film for a TEG. The addition of the two fillers is shown to form discrete networks, which enhance the effective filler-matrix interface leading to a superior electric output (112 V at 13 wt% for both fillers). Li *et al.*[36] have produced a flexible transparent TEG based on a PDMS-poly(tetrafluoroethylene) (PTFE) composite film, which provides a three-fold enhancement in the electric output (95 V) compared to a pristine PDMS-TEG. This enhancement is attributed to an increase in surface potential and a reduction in work function, owing to the addition of the PTFE.[36] In another study, the addition of a MOF, HKUST-1 ($Cu_3(BTC)_2$ where BTC corresponds to 1,3,5-benzenetricarboxylate or trimesate), into a PDMS matrix shows improvements in electrical performance by a factor of 13 (an effective generated power of up to 3.17 mW at a load resistance of 10 MΩ), at a relatively high humidity (10%).[34] Here, the enhancement is attributed to the adsorption of the HKUST-1 to water molecules, which impacts both the electron-trapping and the dielectric constant. These select studies have demonstrated that the introduction of additives into the PDMS matrix, or onto the PDMS surface, can significantly enhance the electric performance of TEGs by increasing the bulk dielectric constant or promoting charging on the contact surfaces.[41]

3.4. Mechanisms of Contact Electrification

The long-standing, and unresolved, issues in understanding the mechanism of CE are a barrier to the fundamental understanding of the systems.[2] In particular, the

identification of the charge carriers and the inherent transfer mechanism during CE still remains a scientific challenge. The CE mechanism between two metal layers, for example, is well understood, whereby electrons are the primary charge carriers and thus the process is called the electron transfer mechanism. In this instance, electrons shift from the metal with the lower work function to the metal with the higher work function at the time of contact between the two layers, and this transfer ceases when the distance between the two surfaces is too large for tunneling. However, for dielectric materials, and even for metals with an outer oxide layer, a significant energy barrier must be overcome for electron transfer to occur. Fundamentally, the band model is often employed to explain the electron transfer during CE in such materials, namely the excitation of electrons by frictional energy.[42, 43]

Recent advancements in advanced surface characterization techniques have enabled the robust experimental evidence of the transfer of ions between surfaces, showing that this can contribute to triboelectric charging, termed the **ion transfer mechanism.**[44] This ionic transfer can occur through multiple sources, which are either intrinsic to the material, or dependent on the environmental conditions (Figure 4(a-c)). In the former scenario the ions are intrinsic in the material, for example, mobile ions in polymers containing covalently bound counterions.[45] In the latter case, the ions are induced by the ambient environment, for instance hydroxide ions in a humid environment can adsorb onto the materials surface and therefore be responsible for electrification[46] (Figure 4(c)).

The driving force of ion exchange in the ion transfer mechanism can be explained by the difference in binding energies.[45] Experiments by McCarty *et al.*[45] have demonstrated the variation in binding strengths between ions and material surfaces results in triboelectric charging, whereby the weakly bound ions transfer to the opposing surface, leaving the strongly bound ions on the original surface (Figure 4(a)).

Additionally, the ambient moisture can play a significant role in CE, especially in the ion transfer mechanism demonstrated in Figure 4(b) and (c). Therefore, water is often used to assess whether ion transfer is the dominant mechanism in TE.[46] The "water bridge" formed upon contact allows for ion migration between the two surfaces and acts as a source for hydroxide ions, leading to charge separation.[45] However, water with a sufficiently high ion content can lead to electrical discharge (or shorting) of the charged surfaces.[45]

Both the electron transfer and ion transfer mechanisms require contact between two dissimilar materials for charge transfer to occur. Historically, this has led to the assumption that all CE requires two different materials with differing physical and chemical properties, and that the magnitude of surface charge is proportional to the

real area of contact. These assumptions have been challenged by a series of studies by Grzybowski *et al.*,[47-49] which has led to the discovery of the material transfer mechanism. This will be reviewed in more detail in the following section.

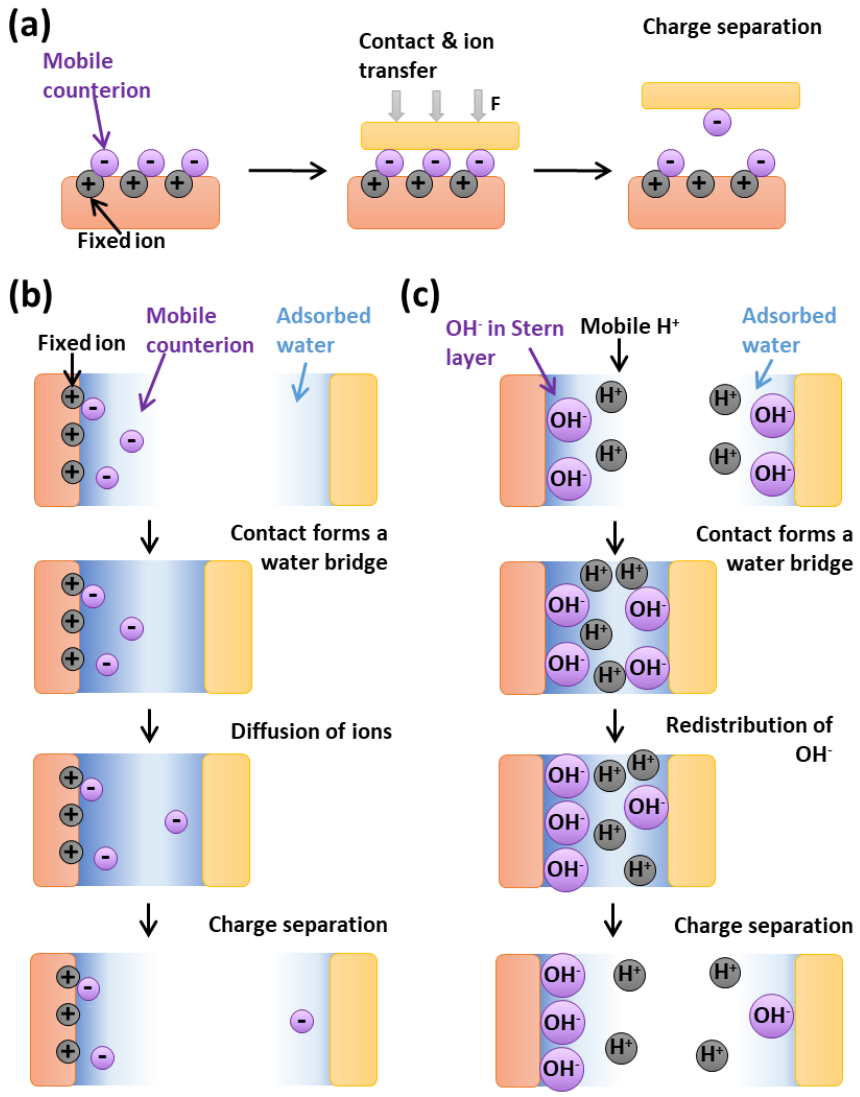

Figure 4. (a) Schematic demonstrating charge separation via the ion transfer mechanism; (b, c) demonstration of the role of water in the ion transfer mechanism of CE for (b) mobile ions flowing through a connected water bridge; and (c) water acting as a source of OH^- with the subsequent redistribution of OH^- and H^+ ions. Adapted with permission.[45] Copyright 2008, WILEY-VCH.

4. Comparing different contact electrification mechanisms

Initially, the argument surrounding the mechanisms of CE focused on what was the specific charge carrier transferred between materials. Electrons, ions, or material segments were all examined, as highlighted previously. The long-standing debate of which mechanism dominates between electron transfer and ion transfer has been recently complicated by the emergence, and increasing significance, of the material transfer mechanism. This section will examine the recent literature and discuss the relevance of the material transfer processes in relation to CE.

4.1. Electron transfer versus ion transfer

4.1.1. Models describing the electron transfer mechanism

The mechanism of CE in the metal-dielectric case has long been proposed to be dominated by electron transfer and generally explained by a surface states model of metals and dielectric materials.[11] The surface states model defines the transfer of electrons during contact of two differing materials, shifting from materials with higher energy states to those with lower energy states (Figure 5, (a)). The transferred electrons remain on the surface of dielectric materials as bound charges, unable to flow freely due to the low conductivity. This model can be similarly used to explain the electron transfer mechanism in the case of dielectric-dielectric CE. [11]

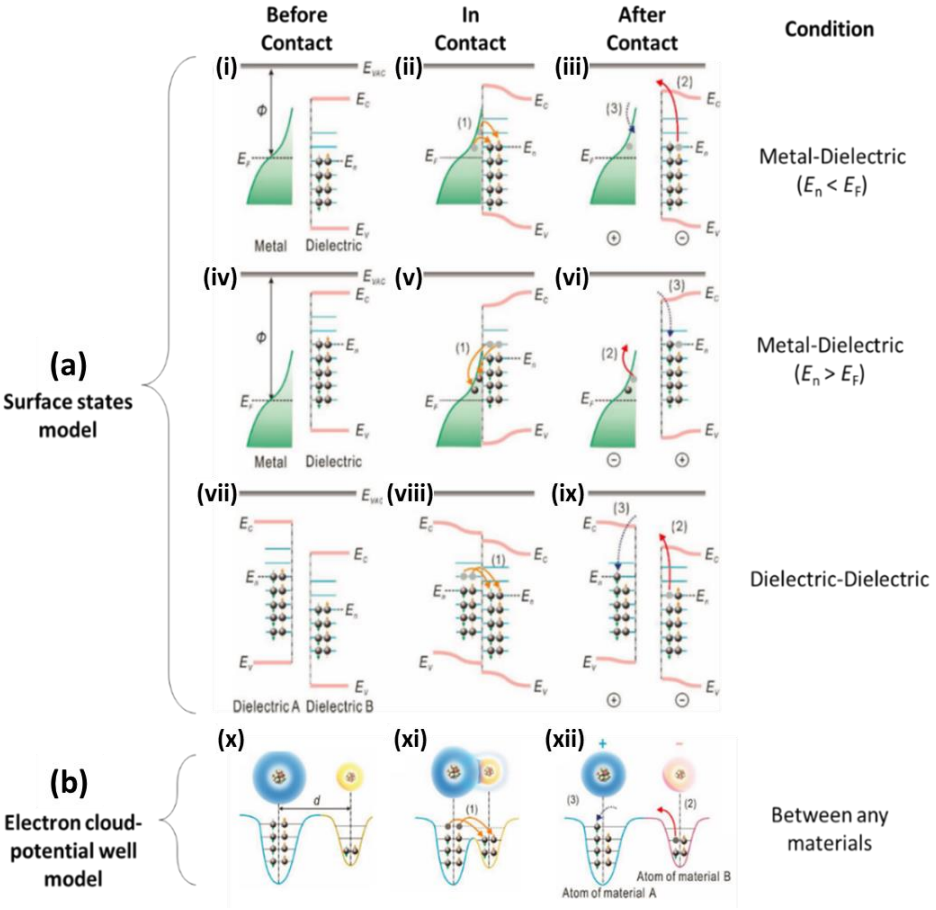

Figure 5. Schematic showing the CE electron transfer mechanism, explained by (a) the surface states model or (b) the electron cloud-potential well model, tracking the charge transfer (left) before contact, (center) in contact, and (right) after contact. (i)-(iii) The electron transfer between a metal and a dielectric if the neutral level of surface states (E_n) is lower than the Fermi level (E_F); (iv)–(vi) between a metal and a dielectric if E_n is higher than E_F; (vii)–(ix) between two different dielectrics; (x)-(xii) between two atoms of any two solid materials that cannot be simply described by a band structure model. Adapted with permission.[11] Copyright 2018, WILEY-VCH.

As the electronic structure is difficult to represent for a range of materials with differing properties, a more gen-

eralized model explaining CE on the atomic and molecular levels has been recently proposed by Xu *et al.*,[11] termed the electron-cloud-potential-well model (Figure 5, (b)). This model originates from a study of CE between a probe and a silica surface in a typical dual-pass Kelvin probe force microscopy (KPFM) measurement during the tapping-mode topography scan pass, which observes electron transfer only if the tip is in the repulsive regime.[50] In the proposed model, electron transfer occurs when two surfaces are brought close enough such that the interatomic distance between the materials is shorter than the normal bond length. The role of the contact force is to then induce a strong overlap between the electron clouds of the two atoms from separated surfaces such that the energy barrier for electron transfer is lower. The model has been further supported by a quantum-mechanical calculation of the electron transfer between different atoms using Einstein rate equations.[51] More recently, Pan and Zhang have provided a detailed mathematical explanation of electron transfer – with preliminary experimental validation.[52] Their proposed model focuses on triboelectric material pairs where one material is a metal, however with further derivation could be applied to more fully understand barriers to electron transfer in polymer-polymer systems.[52]

Furthermore, the electron-cloud-potential-well model has been used to explain the experimentally measured effects of temperature and surface curvature on CE.[53, 54] The friction during contact has been proposed to induce temperature differences between the two layers, leading to thermal excitation of electrons and their subsequent transfer to the material with reduced temperature.[53] Moreover, the surface curvature can induce a change in surface energy, leading to electron transfer from a concave surface to a convex surface between materials with identical composition.[54] However, silica (a semiconductor) is used to model dielectric materials in these studies, rather than dielectric polymers, as the electronic structure of semiconductors can be easily represented by energy bands. In polymers, the effective 'band-gap' is significantly higher than silica. Thus, the extent of electron cloud overlap induced by contact forces remains a matter of controversy when discussing results from CE or TE experiments using polymer systems.

4.1.2. The Debate: Which is the Dominant Mechanism?

Although the dominant mechanism of CE is still in debate, Wang and Wang[55] have proposed that electron transfer is the dominant mechanism for TE between solid-solid pairs and for initiating TE in general. One traditional way to confirm which mechanism dominates is to correlate the ordering of the triboelectric series to the very basic properties of the materials. Over the years there have been many different versions of the triboelectric series proposed, primarily due to a mismatch in testing methods. Recently, a universal method for accurately

measuring the triboelectric performance of various materials, in a strictly controlled environment, has been proposed.[56]

However, even if a uniform ordering of the triboelectric series could be reproduced by different researchers, all following the same standard protocol, there is still doubt as to whether the ordering will represent the true nature of the materials. Nevertheless, while Wang and Wang[55] argue electron transfer is the dominant, if not the exclusive, mechanism for CE, some research groups argue that electron transfer cannot explain the triboelectric series of polymers.[57]

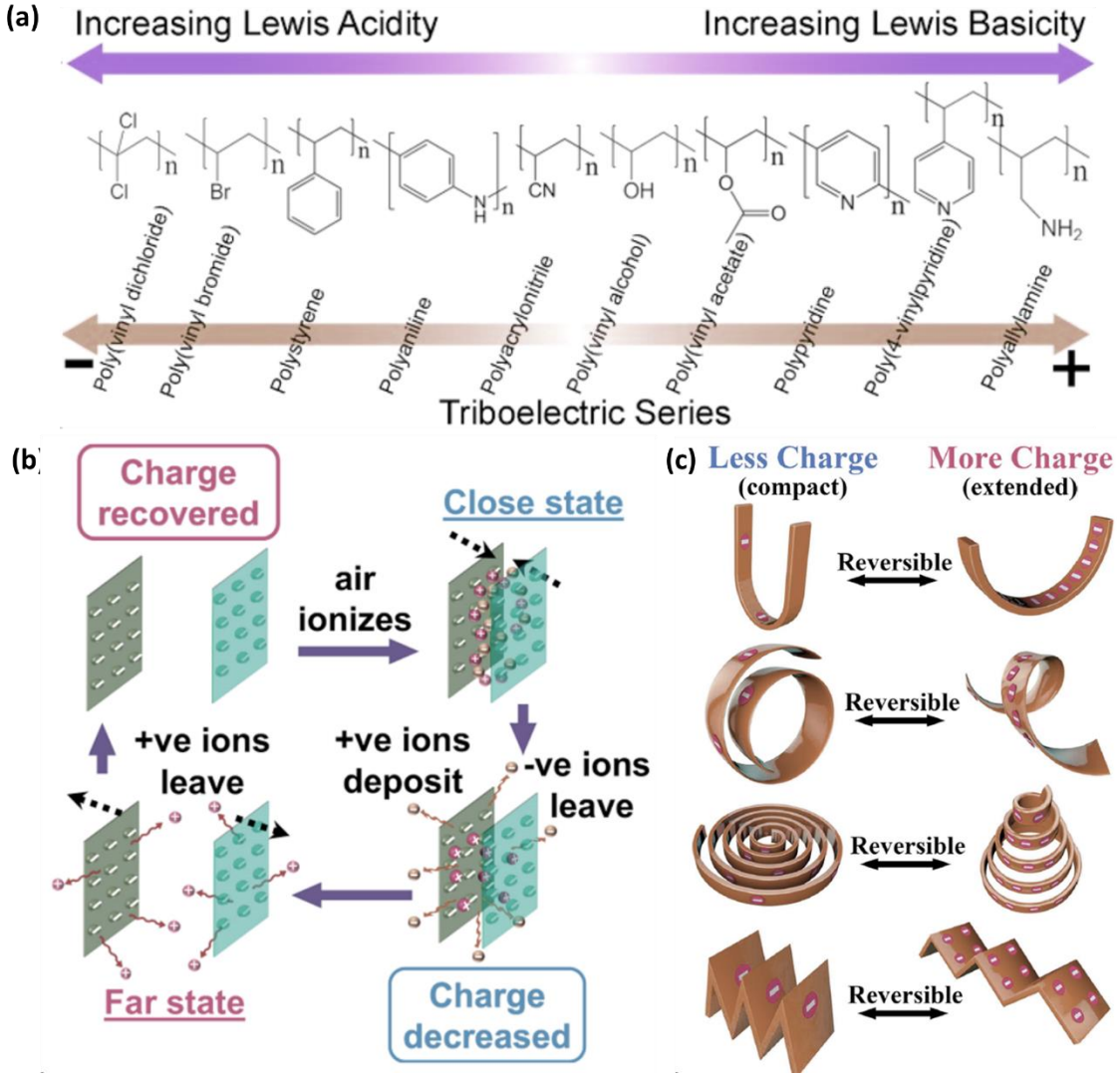

Figure 6. (a) Schematic comparing the experimentally-derived ordering of materials in the triboelectric series and their Lewis basicity/acidity (Reprinted with permission.[57] Copyright 2019, American Chemical Society.); (b) Schematic illustrating the proposed mechanism for the reversible change in charge of two initially negatively charged surfaces as the separation between them is varied (Reprinted with permission.[58] Copyright 2017, American Chemical Society.); and (c) Schematic illustrating materials with differing geometry undergoing conformational changes when subjected to external forces (e.g., bending or twisting). Reprinted with permission.[59] Copyright 2020, American Chemical Society

Zhang *et al.*[57] have proposed a reason why there is a lack of comparative results in the triboelectric series, arguing the development of the series uses a metal as the contact reference. A metal reference is thus deemed problematic in the case of contact between two polymeric materials. The authors have used exhaustive empirical testing of a multitude of polymer pair combinations, ordering each polymer based on the sign and magnitude of the relative surface charge between the pairs. They observe the ordering strictly correlates to the Lewis basicity of the polymers (Figure 6, (a)), whereas the ionization energy, dipole moment and dielectric constant do not affect the ordering of the series. Thus suggesting that the fundamental mechanism of CE is ion transfer, as opposed to electron transfer.[57]

4.1.3. More complexity brought by ion movement

Generally, the ion transfer mechanism proposed for electrification involves the movement of ions between two triboelectric layers. However, the real-time surface charge can also be affected by ion exchange from the surface to its surrounding air. This has been proposed by Pandey *et al.*,[58] demonstrating the reversible reduction in surface charge as the distance between two similarly charged (i.e., both positive or both negative) surfaces decreases. The authors proposed a mechanism to explain the dependence of surface charge on the distance between the two charged surfaces (Figure 6, (b)): as the two surfaces are brought close to each other, the increasing electric field ionizes the air and consequently generates mobile gas ions. These mobile gas ions deposit onto surfaces charged with opposing polarity thus reducing the measured surface charge. As the surfaces are separated, and distance between the two surfaces increases, the mobile gas ions desorb from the surface due to the decreased electric field. Subsequently, these ions can recombine back to air, allowing the two surfaces to revert to their original surface charge. This phenomenon does not play a significant role in the operation of simple TEGs with two parallel triboelectric layers, which do not undergo significant shape change during the entire compression-separation motion. However, this phenomenon may affect the output performance of TEG devices stacked in complex geometries or those which undergo severe changes in shape during operation (Figure 6, (c)).[59]

4.2. What role does material transfer play in the triboelectric effect?

Research has focused on understanding how the electron and ion transfer mechanisms occur in both CE and TE, yet there remains very few studies focusing on factors that would affect the material transfer mechanism. Thus, understanding the magnitude and role of material transfer in TEG devices is not trivial. Despite the multitude of reports correlating material transfer across surfaces, contact, friction, and charge,[16, 60-64] material transfer is often overlooked in TEG literature and contributions from material transfer to TE erroneously attributed to the electron transfer mechanism.

4.2.1. Discovery of material transfer in the triboelectric effect

Initially, both the electron and ion transfer mechanisms have assumed the requirement for contact be-

tween dissimilar materials. Apodaca *et al.*[47] have demonstrated that these assumptions were incorrect by observing TE between identical materials (i.e., both surfaces consist of PDMS) (Figure 7, (a)), and have proposed that TE is inherently driven by the fluctuation of surface composition or structure of the material at the molecular level (Figure 7, (b)), supported by theoretical calculations.[47] The authors speculate that the electron transfer from the donor oxygen sites to acceptor silicon sites in PDMS is the origin of TE. Subsequently, this molecular-level fluctuation in oxygen and silicon components translates into the macroscopic TE of two identical PDMS surfaces with inherent molecular-level asymmetry. This fluctuation in local composition has been further visualized as a random "mosaic" of oppositely charged patterns by Baytekin *et al.*[48] The authors, for the first time, have experimentally demonstrated the existence of charge mosaics for identical materials. Further, they have scrupulously excluded the possibility of the observed mosaics arising from imperfect contact, by using the conformal contact between two flat PDMS films. The authors have also experimentally confirmed the existence of material transfer during TE by confocal Raman microscopy (Figure 7, (c)) and X-ray photoelectron spectroscopy (XPS) studies. This mosaic pattern arises from the heterolytic bond cleavage of PDMS, via the detection of oxidized species, formed by the reaction between the PDMS fragments and the oxygen species in the atmosphere (oxygen or water). In a more recent study, mosaic patterns of positive and negative surface charges produced by TE have also been found to occur in dissimilar materials between metals and polymers (including PDMS).[65]

Baytekin *et al.*[49] have further confirmed the significance of material transfer through the observation of polarity reversal in TE under repeated contact-separation motion. The authors attribute the polarity reversal to bi-directional material transfer, detected by KPFM, observing minimal material transfer when the relative softness of the two polymer triboelectric layers is low.

These studies have conclusively demonstrated the correlation between the local PDMS composition, which relates to the material transfer in CE, and the resultant charge generation, thus providing additional insights into how elastic and topographical characteristics can affect TE.

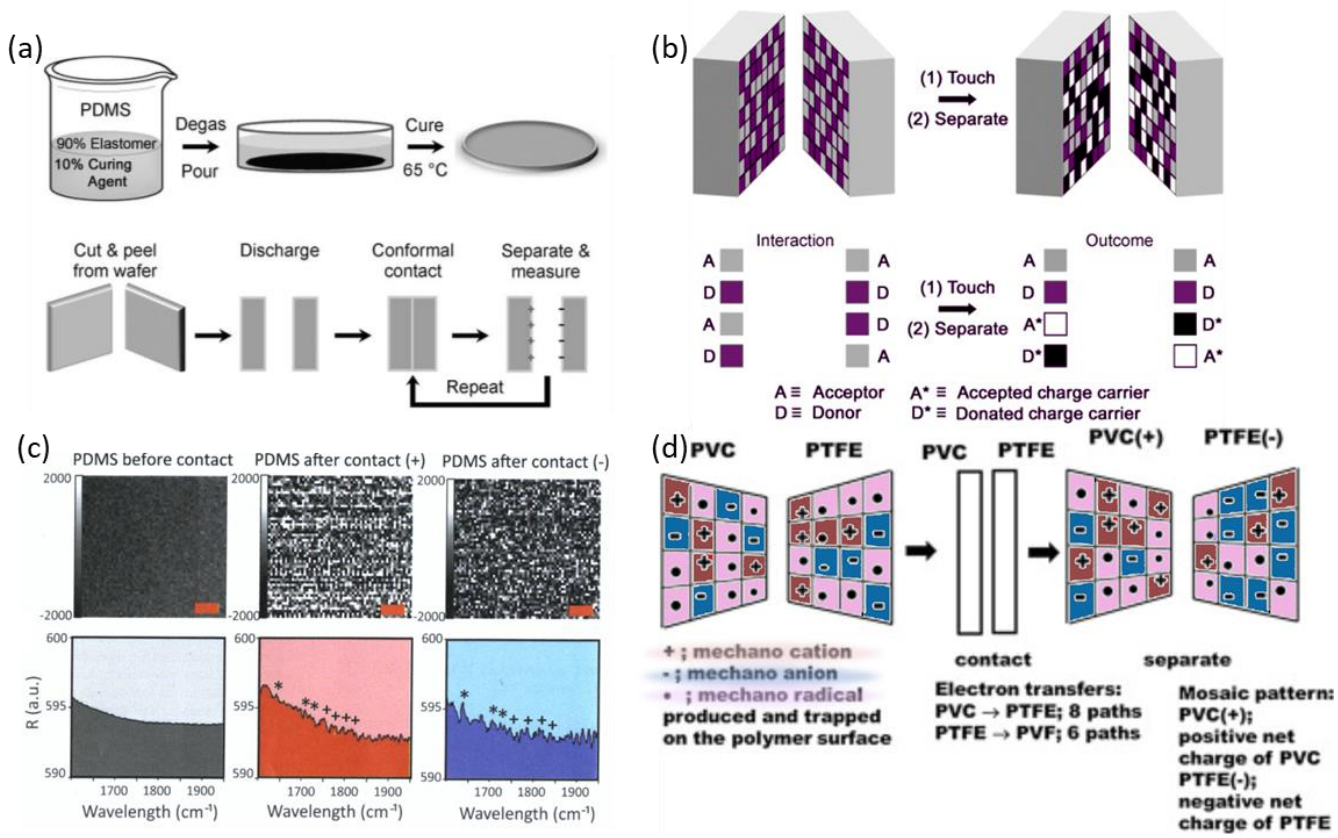

Figure 7. Schematics overviewing the material transfer mechanism. (a)-(b) Observation of TE between PDMS films with identical composition, suggesting charge transfer from donor to accepter due to the local spatial fluctuation of surface atoms. (a) Experimental procedure of PDMS film preparation and contact-separation of the identical PDMS films; (b) The theoretical model proposing charge transfer occurring between contacting donors and acceptors. Reproduced with permission.[47] Copyright 2010, WILEY-VCH. (c) Experimental evidence of TE due to fluctuations in local composition: the charge "mosaic" - confocal Raman microscopy image and its corresponding total Raman spectra of the regions mapped in the image ($SiCH_2COOH$ marked with *, SiCOOH and RCOOOH where R=Si or C marked with +). Reproduced with permission.[48] Copyright 2011, American Association for the Advancement of Science. (d) Proposed electron transfer among mechano-anions, mechano-cations and mechano-radicals produced by material. The random mosaic pattern with an oppositely charged nanoscopic domains on the surface of PVC and that of PTFE are produced by mechanical fracture of covalent bonds comprising the main chain of polymers on the surface. The electron transfer paths from mechano-anions or mechano-radicals mechano-radicals or mechano-cations under contact on the surface (shown in the center). After separation, a new different random mosaic pattern is produced. Reproduced with permission.[66] Copyright 2014, Elsevier.

Subsequent studies have probed the role of intermolecular forces (cohesion forces within the material and adhesion forces between different materials) by conducting TE between identical materials.[61] A variety of flat polymer samples were investigated with similar surface roughness but different physicochemical properties, observing that the polymers with lower moduli generated greater charge during TE relative to polymer with higher moduli. Additionally, TE experiments between polymers with the same difference in modulus showed similar surface charge regardless of the absolute modulus of the polymers used (Figure 8, (a)i). Thus, as modulus is directly proportional to the cohesive energy of the material, these experiments infer that polymer cohesion energy possesses greater influence on TE relative to the differences in the physicochemical properties of the materials.

In order to eliminate physicochemical influences, and provide definitive evidence of the cohesive energy influences on TE, experiments have been undertaken on pristine PDMS with varying degrees of cross-linking (Figure 8, (a)ii-iii). Here, only the modulus difference between

sets of two PDMS sheets was varied through the degree of cross-linking, removing compositional variations. A ten-fold difference in the generated TE charge was observed between the PDMS set with low modulus difference and the PDMS set with high modulus difference, whereby the latter demonstrated the greater charge generation capability and thus confirmed the significant role of cohesion energy in TE. Further experiments on the modification of the adhesion between interfaces have demonstrated a similar effect, whereby a greater adhesion between two contacted surfaces has resulted in an increase in surface charge generation. Hence, the increase in surface charge with stronger surface adhesion and lower bulk cohesive force confirms that covalent bond cleavage (i.e., material transfer) is the primary mechanism for CE in these PDMS systems.

4.2.2. Possible roles material transfer play in the triboelectric effect

The direct consequence of material transfer is the formation of mechano-radicals, mechano-cations and mechano-anions due to bond cleavage. How these mechano-radicals/ions participate in TE, giving rise to net charge on two surfaces or induce further electron transfer, is a key question to be answered, and thus will form the basis of discussion in this section.

4.2.2.1 Mass transfer promoting electron transfer

Generally, without material transfer, the donor and acceptor sites for electron transfer are neutral atoms and are identified by electron affinity. However, mechano-radicals and mechano-ions are formed during material transfer. Sakaguchi *et al.*[66] have assigned mechano-anions as donors, mechano-cations as acceptors, with mechano-radicals able to act as both donors and acceptors (Figure 7, (d)). This model, assuming electron transfer between mechano-radicals and mechano-ions formed *via* material transfer, could successfully predict the triboelectric series based solely on the chemical structure of two triboelectric materials. [66]

This secondary charge transfer of electrons between mechano-radicals and mechano-ions is crucial to understand the overall picture of TE.

4.2.2.2 Acting as bulk ions charging

The mechano-particles created by material transfer can not only act as better sites for electron transfer but can also be considered as bulk ions transferred across surfaces, thus charging the surfaces by the ion transfer mechanism. Yun *et al.* have demonstrated TE between a gold foil and a patterned PDMS film, mapping the electrostatic charge on the Au by KPFM and showing the same pattern on the Au foil as the patterned-PDMS film.[67] This finding indicated the presence of ion migration, as the charge should be uniformly distributed if electrons were transferred across (Figure 8, (b)). In their work, the authors refer to the charge carrier as an ion. However, it is an ion with multiple atoms that is generated via bond cleavage of the polymer, rather than a typical ion as that described in the ion transfer mechanism.[67]

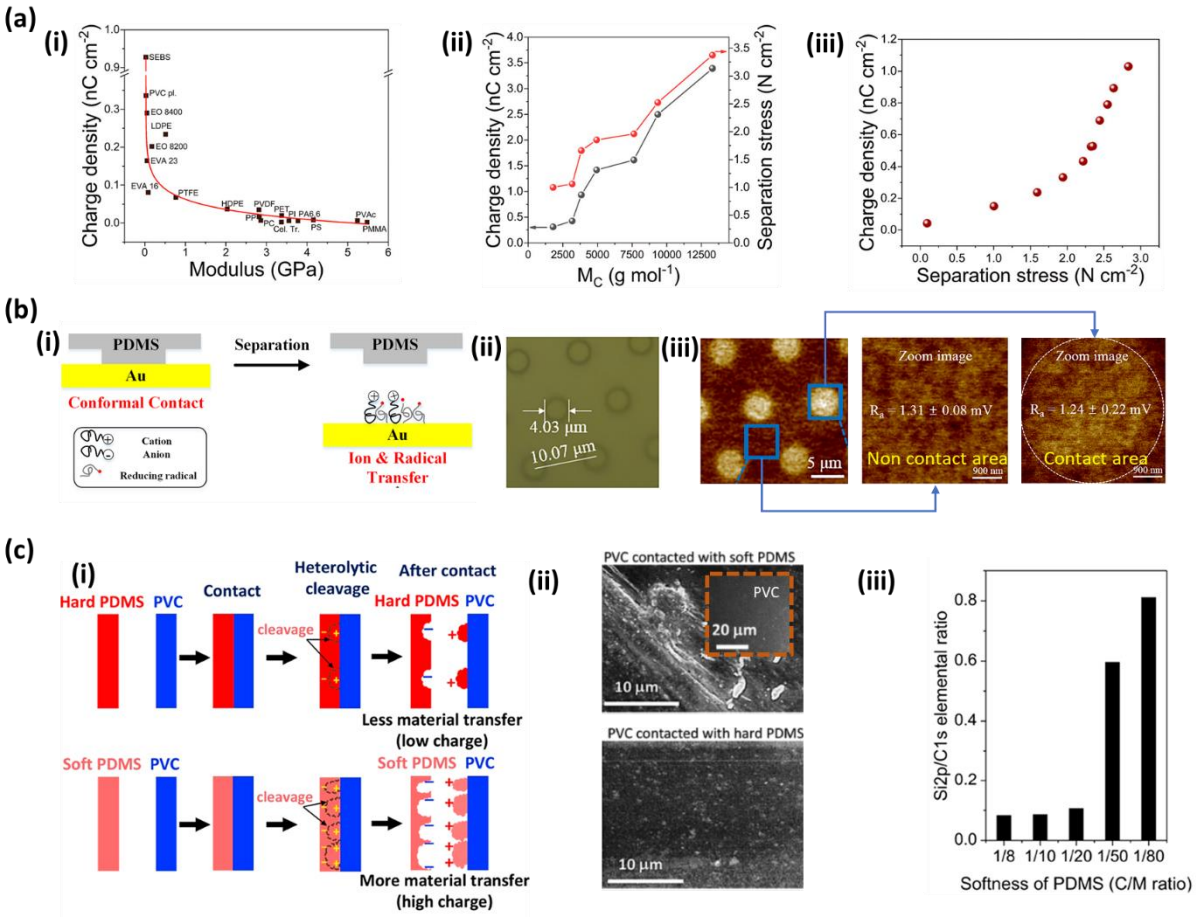

Figure 8. (a) Material transfer between identical polymers; (i) Correlation between the modulus of polymer material and surface charge; (ii) Surface charge density and adhesion force increase with increasing MW between PDMS crosslinking points; (iii) Relationship between the charge and separation stress required when the contacting force before separation step is gradually increased for PDMS (10: 1 ratio). (i)-(iii) Reproduced with permission.[61] Copyright 2019, The Royal Society of Chemistry; (b) Material transfer between PDMS and Au. (i)-(iii) Adapted with permission.[67] Copyright 2018, American Chemical Society. (i) Illustration of the proposed mechanism for CE; (ii) Optical image of dot-patterned PDMS; (iii) Potential map of Au after contact of the dot-patterned PDMS with zoom images of contacted and noncontacted areas. (c) Material transfer between PDMS and PVC (i) Illustration of material transfer and charge transfer occurring simultaneously during the CE of two materials. (ii) SEM images of PVC before (inset) and after contact with soft/hard PDMS; (iii) correlation of XPS Si and C signal with PDMS curing ratio. (i)-(iii) Reprinted with permission.[18] Copyright 2018, American Chemical Society.

Recently, the significance of material transfer has been investigated, by correlating the amount of mass transfer with the generated surface charge (Figure 8, (a),(c)).[18] Notably, the charge density was related to physical properties of modulus, molecular mass, and separation stress, showing a softer, higher molecular mass polymer lead to increased surface charge density. This is understood by an increased degree of chain entanglement at the interface during contact-separation leading to increased mass transfer and heterolytic bond cleavage (Figure 8, (a)). [61]

Spin-coated PDMS films, with varying degrees of softness, were brought into contact with a PVC film (as a reference material). The material transfer of PDMS onto the PVC film was quantified by an increase in surface roughness of the PVC surface after each contact. The presence of PDMS on the PVC surface after contact was observed in scanning electron microscopy (SEM) images (Figure 8, (c)ii) and the PDMS Si 2p/C 1s ratio in XPS analysis (Figure 8, (c)iii). Importantly, the authors report a six-fold increase in the charge transfer as the degree of softness in-

creased, correlating to the magnitude of material transfer. This correlation between material transfer and charge transfer is described by: (1) heterotic cleavage of PDMS molecular bonds within the bulk polymer, resulting in charged fragments and (2) the transfer of smaller surface oligomeric PDMS fragments onto PVC.[18] Consequently, the strong adhesive force and the weak inherent strength of the material are the key contributors to the facilitation of charge transfer *via* bond cleavage.

In both instances demonstrated above, the charged fragments of PDMS (i.e., the bulk ions) are transferred to the secondary material primarily due to a greater attraction to the secondary material. However, despite the strong relationship between material transfer and charge transfer shown here, it remains unclear what determines the polarity of the two contacting materials. In both instances, the PDMS possesses a negative charge following contact, implying the majority of the transferred PDMS fragments are cationic. One possible explanation for this phenomenon is that the heterolytic cleavage results in two mechano-ions with different sizes, and while the electrons transfer to the larger mechano-ion, the smaller mechano-ion will generally transfer to the secondary surface. Notably, it is yet unclear whether this heterolytic cleavage process is reversible.

4.3. Factors influencing the dominant charge transfer mechanism

As the understanding of the role of material transfer has developed within the scope of TE, it has become evident that the dominant mechanism is largely dependent on the specific experimental parameters. In this section, we will discuss the current state of the art in how these conditions impact the TE mechanism.

4.3.1. Effect of combination of material pairs

The TE mechanism in metal/polymer pairs is largely dependent on the surface potential barrier height, thus the dominant mechanism is electron transfer. The surface potential barrier height, derived by applying the Richardson's Law and based on the decay of static charge due to thermionic emission, can be used as an indicator for identifying the dominant mechanism in TE.[68] Conversely, for TE of polymer/polymer pairs, the surface potential barrier height can be related to multiple factors, indicating the co-existence of both electron transfer and material transfer mechanisms.[68] Xia *et al.*[68] have proposed a material-dependent charge transfer mechanism where the TE in metal/polymer pairs follow the commonly accepted electron transfer mechanism, while polymer/polymer pairs follow a simultaneous electron, material and ion transfer process.

4.3.2. The effect of water

The existence of a water layer on solid surfaces, formed under a humid atmosphere, further complicates the understanding of TE. Table 1 summarizes the possible roles of water during the contact-separation motion of a solid-

solid TEG. The presence of water can promote CE, as it can act as an ion source (e.g., H^+ and OH^-),[45] and also form an electric double layer.[69] However, conversely, as a neutral molecule, water can hinder the CE process by forming a layer between two solid surfaces[45] and subsequently exchange electrons with the solid surface.[70] Additionally, the relatively high dielectric constant of water can stabilize the generated charge and therefore hinder the CE process.[46] Overall, it is currently difficult to definitively conclude whether the existence of water will promote or suppress surface charge generation, even though it is usually assumed without detailed studies that hydrated ions are the major charge carriers in the solid-liquid systems.

Recently, studies have focused on the liquid-solid interface to investigate whether ion transfer or electron transfer is the dominant mechanism underlying CE. Nie *et al.*[69] have studied the CE process between PTFE and deionized water experimentally, and by theoretical calculations. The value obtained for the charge induced by OH^- ions near the interface with PTFE experimentally, is ten-fold larger in relation to the calculated value, inferring the remaining difference in charge can be attributed to electron transfer. The authors have proposed a detailed mechanism (Figure 9(a)), where electron transfer between PTFE and water, under compression, was responsible for charging the surface, with adsorption of H^+ and OH^- ions only playing a minor role. Similar experimental results have been obtained by Lin *et al.*[71] in further identifying the relative contributions of electron transfer and ion transfer to liquid-solid CE. The authors have investigated, at elevated temperatures, the charge decay of a silica surface after triboelectric charging by water. This approach exploits the relative ease of electron emission in thermionic emission relative to ions, which remain adhered to the surface. The experiments, performed on a variety of samples, compare the effect of surface hydrophobicity, the concentration of ions in water, and the pH of the solution. The authors propose a two-step model (Figure 9(b)) for the mechanism of liquid-solid CE.[71] In the first step, the close contact between water and the surface enables the electron transfer to the surface from the water molecules, imparting negative charge to the material surface. The authors attribute this phenomenon to the overlap in electron clouds between the two materials, based on the electron-cloud-potential-well model also proposed by the same group.[72] In the second step of the liquid-solid CE mechanism, positive ions in the water are consequently attracted to the negatively charged surface, thus forming an electric double layer (Figure 9).

Table 1. Effects of water presence during the contact-separation motion of a solid-solid TEG.

Possible roles of water during the contact-separation motion of a solid-solid TEG	Ref.	Effect on TE
Formation of a shield layer - blocking effective contact between two solid surfaces	[45]	Reduction
Electron transfer from water to tribonegative solid surfaces	[70]	Enhancement

EDL formation of trace H^+ and OH^- ions, screening electrification	69	Reduction
Adsorption of trace OH^- ions on solid surface, charging by ion transfer	45	Enhancement
Stabilization of surface charges developed during CE due to increases in dielectric constant	46	Reduction
Alternation of the solid surface through reaction with mechano-radicals		Unknown

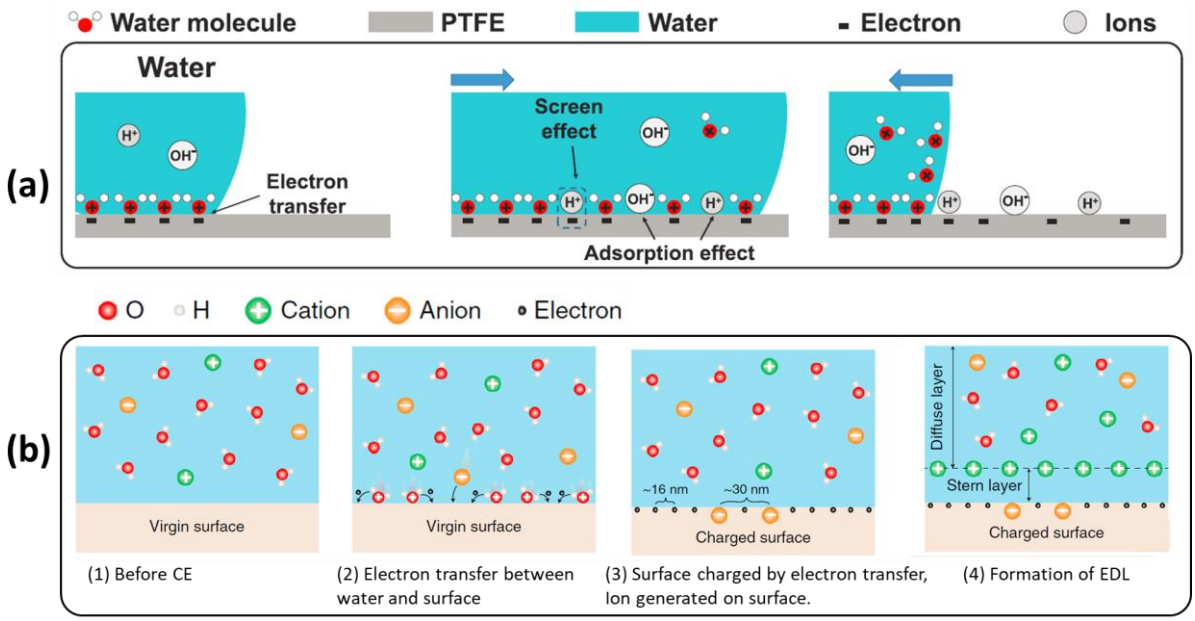

Figure 9. The mechanism of CE between water and solid surfaces. (a) Demonstration of the effect of removing water from the surface, thereby stabilizing surface charge by leaving behind adsorbed ions. Reproduced with permission.[69] Copyright 2019, WILEY-VCH. (b) Demonstration of the effects of water remaining on the solid surface, stabilizing surface charge through the formation of an EDL. Adapted from Shiquan Lin et al., via Creative Commons CC BY license, Copyright 2020, Springer Nature.[71]

We have now demonstrated that CE is highly dependent on the materials used, the amount of water, and the interfacial adhesion. While there is often a dominant mechanism, understanding CE for a given system must incorporate the understanding of electron, ion, and material transfer, as well as how the contribution of each varies in accordance with the operating conditions.

5. Improvements in triboelectric performance of poly(dimethylsiloxane)

Whilst debate is ongoing around the dominant charge carrier species (electrons, ions, or material fragments), further research is being undertaken on the engineering aspects of improving TEG devices. Currently, the primary aim in these efforts is the enhanced contact between the triboelectric layers. Improving contact between triboelectric layers enables increased friction, subsequently leading to increased charge separation, as well as promoting charge transfer through all three mechanisms. This improved contact results in: (1) the reduction in the tunneling distance for electron transfer, and (2) an increased

adhesive force between the layers, enabling bond scission and/or the transfer of mobile ions.[63, 64, 73]

In general, the larger asperity of a rough or patterned surface will possess a greater triboelectric contact area relative to a flat surface, when normalized to the geometric area. Hence, the contact area can be increased by improving the asperity *via* surface patterning, with reduced feature dimensions leading to a larger effective contact area.[74]

5.1. From Micro- to Nano-scale Topographies

The effect of surface patterning has been previously studied on PDMS/polyester TEGs.[8] The micropatterns on the PDMS side (negatively charged) have been generated by casting PDMS onto a patterned Si wafer mold, while the polyester side (positively charged) has remained flat. Multiple geometric patterns were tested (Figure 10, (a)), including raised lines, cubes and pyramids. This study has observed that a pyramid pattern with sharp tips provides the greatest performance (18 V) relative to flat tips (15 V). Additionally, increasing the roughness leads to increased performance for a pattern with the same geometric features. Subsequently, the use of replica molding has become commonplace to create surface patterns, with a primary focus on decreasing the feature dimensions to the nanoscale such that the surface roughness is increased.

Jang *et al.*[20] have created a hexagonal close-packed structure with a controlled feature size on top of a spin-coated PDMS film. The micropattern is formed by rubbing polystyrene (PS) colloids onto the PDMS film, thus forcing them to form a monolayer of close-packed colloids. Here, the dimensionality and periodicity are controlled by modulating the particle size of PS colloids (1 μm, 2 μm and 5 μm). The authors have further suggested this mold is suitable for intaglio and embossed PDMS microstructured films.

Further work has produced dual-embossed PDMS structures with nanoscale dimensionality, through a replica mold containing anionic PS colloids with a diameter of 800 nm (Figure 10(b)). The TEG, with a tribonegative layer consisting of nanopatterned PDMS and a tribopositive layer consisting of aluminum foil, has demonstrated a significantly improved performance (intaglio = 103 V, dual embossed = 207 V) relative to a flat PDMS film (flat = 57 V).

Pillar patterns have also been produced on the nanoscale in an attempt to increase the periodic surface roughness. The nanopillar-array architecture of the PDMS layer (NpA-PDMS) was fabricated by casting PDMS into a nanoporous anodic alumina template (Figure 10(c)).[21] For the greatest electric performance of the NpA-PDMS TEG, the spacing between the patterns of NpA has been optimized. The authors observe a maximum performance at minimal feature spacing, suggesting that increased contact area is not the primary driving force for the performance increase. An optimized perfor-

mance has been observed in the NpA-PDMS with a period (inter-pattern spacing) of 125 nm and nanopillar diameter of 60 nm, with an open-circuit voltage of 568 V and a current of 25.6 μA under 10 N of applied force. COMSOL simulations have demonstrated the peak contact force (effective/uniaxial stress x contact area) occurs at an intermediate spacing. Therefore, the authors have concluded that both the stress on the contact surface and the contact area affect the electric performance of the TEG. It should be noted here that keeping the force constant, but not reporting the deformation area can be misleading as the key factor in charge generation is stress, not simply applied force.

A comprehensive analysis on how the geometric shape of microscale surface features can affect the performance of TEGs has been carried out by Choi's group.[75] They have investigated the effects of geometry on the electrical output, durability and force sensitivity. Two shape-types, pillar and dome, were patterned on soft PDMS with identical height (245 nm) and diameter (500 nm). The opposite surface consisted of a rigid Au layer, which deformed the soft PDMS under applied mechanical stress. Both the pillar- and dome-based TEGs showed almost identical electrical performance under a low applied force; however, the dome-shaped TEG exhibited greater sensitivity at higher force. Conversely, the charge generated by the pillar-shaped TEG rapidly saturated at increasing applied force. Finite element analysis simulations were also performed to study the deformation of the two shapes under an applied force, demonstrating that the dome-shape deforms into a flat surface when compressed by the rigid Au layer, with an increase in the surface area as the applied force increases. In contrast, the pillar-shaped TEG does not deform to create a flat surface, and subsequently does not exhibit an increase in the contact area. Further, the simulations revealed a significantly greater stress concentration occurring at the top of the dome-shaped pattern in comparison to that of the pillar-shape pattern. Although the dome-shaped TEG possessed a superior electric performance and force sensitivity, owing to its larger deformation and internal stress, this geometry resulted in decreased durability with a decreased output of 20% after 1 million cycles (pillar-shaped TEGs did not exhibit degradation).[75] The enhancement in electrical performance and degradation is likely attributed to an increase in material transfer induced by the concentrated stress. Consequently, the dome-shape enhances the short-term triboelectrification, however leads to the loss of the defined dome structure with time.

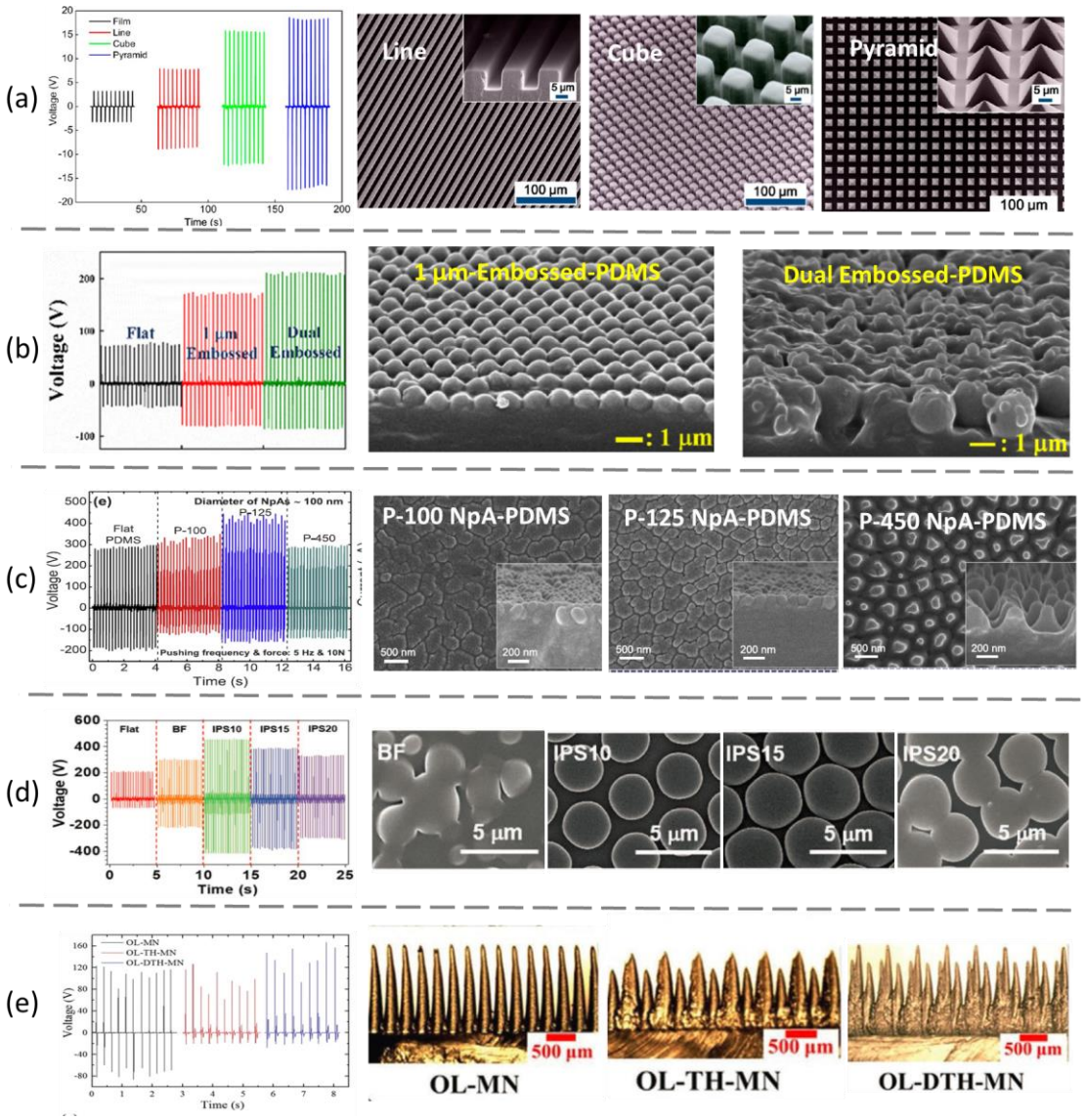

Figure 10. The morphology and electromechanical energy harvesting performance of surface patterned PDMS-TEGs produced by replica molding. (a) Micropatterned PDMS with raised line, cube and pyramid surface geometries (Reprinted with permission.[8] Copyright 2012, American Chemical Society); (b) PDMS patterned using polystyrene colloids (Reproduced with permission.[20] Copyright 2016, Elsevier). (c) Nanopillar PDMS produced through casting over an anodized aluminum oxide template (Reproduced with permission.[21] Copyright 2017, Elsevier.); (d) Biomimetic structures resembling a treefrog's toe cast in PDMS (Reproduced with permission.[22] Copyright 2019, WILEY-VCH.); (e) PDMS microneedles produced with varied aspect ratios and sizes by laser etching (Reproduced with permission.[76] Copyright 2020, WILEY-VCH.)

Hierarchical structures have been created to increase surface roughness. As an example, an argon plasma has been used to impart nanopillar morphology on a micropatterned PDMS replica to form a multilevel structure.[77] Argon plasma treatment induces chain scission on the PDMS surface, generating reactive radicals which form hydrophilic groups (e.g., carboxyl or hydroxyl groups) when exposed to air. The combination of increased surface roughness and reactive radicals resulted in a threefold enhancement of the electrical performance. This improvement was attributed to a larger contact surface area and a lower force being required to compress the submicron-pillar structure. Furthermore, the hydrophobic recovery of the argon plasma-treated PDMS leads to a de-

crease in adsorbed water which, as discussed by Grzybowski *et al.*[46], helps stabilize the surface charges formed during CE. However, considering the weakened chemical bonds generated in the plasma treatment process, an increase in mass transfer between surfaces is likely. This primary mechanism of mass transfer was demonstrated through the reduction of electrical performance as a function of time.

Inspired by treefrog toe pads, a highly ordered hexagonally non-close-packed micropattern has been produced on PDMS (Figure 10(d)), mimicking the strong adhesion these toe pads have to various surfaces in nature.[22] The pattern was produced by casting PDMS on concave films, which were formed by a phase separation method using a volatile solvent/nonsolvent pair to control the surface morphology. Methanol was used here as the nonsolvent to control the separation between the micropattern arrays. This investigation demonstrated an increased electrical performance (from 280 V to 440 V) was achieved with a lower contact area by increasing separation between micropatterened arrays. This contrast between high performance and low contact area highlights the importance of the degree of deformation in the electrical performance of TEGs. As a higher degree of deformation is correlates with the material being under greater internal stress, there is a lower activation energy for bond cleavage in highly deformed samples. Therefore, these patterning approaches that increase the degree of deformation promote lead to increased material transfer and thus measured TE.

Other molds used for creating random or disordered surface patterns include commercially available sandpaper,[78] natural materials,[79] and lab-made thick film[23]. However, although replica molding provides tuneable control of a patterned structure, the process can be very tedious involving multiple steps and nano-scale patterns cannot be created easily.

Carbon dioxide (CO_2) laser ablation is a promising and fast microstructuring tool. Elongated-triangular Al microneedle structures have been fabricated in PDMS using CO_2 laser ablation on a PMMA substrate followed by replica molding (Figure 10(e)).[80] The Al microneedles possessed a high-aspect-ratio, with a base diameter of ~300 μm, and height between 300 μm and 1000 μm, which could be controlled by the laser parameters. An optimized Al/microneedle-PDMS TEG was shown to generate up to 102.8 V of open-circuit voltage and 43.1 μA of short circuit current, corresponding to a short circuit current density of 1.5 μA/cm^2. The high performance of these microneedles is understood by considering the bend-release process of long microneedles during contact-separation. The viscoelasticity of PDMS, coupled to the high aspect ratio of the microneedle shape, results in a low applied force leading to bending, sliding and deformation, thus greatly enhancing the real contact area and friction.

The performance of various surface-patterned PDMS TEGs are featured in Table 2.

Table 2. Summary of the structural parameters and energy harvesting performance of surface-patterned PDMS TEGs.

Process	Comments	Pattern Shape	Dimension	Best Performance	Ref.
Replica Molding	Mold: patterned Si wafers	Lines/cubes/pyramids	Pattern size: ~10 μm	18 V (pyramid; bending mode)	[8]
	Mold: PDMS film patterned by rubbing with PS colloids	Close-packed hemispheres	Diameter: 1-5 μm	207 V (compressive force of 90 N in relative humidity of 20%)	[20]
	Mold: nano porous anodic alumina	Pillars	Diameter: 50-100 nm Height: 150 nm Spacing: 100-450 nm	568 V (10 N of pushing force and 5 Hz of pushing frequency)	[21]
	Mold: concave PMMA produced by phase separation method	Non close-packed pillars	Diameter: ~4 μm	490 V (applied force of ≈38 N at frequency of 5 Hz)	[22]
	Mold: PMMA film patterned by CO_2 laser ablation	Circular cone with high aspect ratio	Diameter: ~1 mm	167 V	[76]
	Mold: polymer films roughed by sandpaper abrasion	Sandpaper-like	Grit size: 0.8-10 μm	200 V (pressure of 80 kPa)	[78]
	Mold: leaf	Leaf-like	Roughness: ~32.1 nm	56 V	[79]
	Mold: porous PE multilayer	Irregular	Pore size: < 5 μm	242 V (compressive force of 90 N in relative humidity of 20%)	[23]
Direct Patterning	Direct patterned by laser	Concave spots	Diameter: ~10 μm	45 V (applied force of 100 N at frequency of 5 Hz)	[19]
	Argon plasma treatment on the mold	Micro pillar arrays	Roughness: ~140 nm	72 V (applied force of 10 N at frequency of 5 Hz)	[77]
	3D printing	Micro/nano hierarchically patterned structure	Pore size: ~10 μm Wall thickness: ~100 nm	55.8 V (applied force of 4 N at frequency of 4 Hz)	[24]

5.2. Complementary patterns

Surface patterning has not only improved in feature size but has also evolved into double-sided patterning. A systematic study on how complementary and contrasting patterns on both layers affect the TEG performance was performed by Han *et al.*[78] Patterns were produced using sandpaper of various grit sizes. The patterned PDMS was made by casting onto sandpaper and subsequently peeling away to produce a rough PDMS surface. The copper patterned surface was produced by sputtering directly onto the surface of the sandpaper, with roughness corresponding to the grit size of the sandpaper. For TEGs consisting of one flat and one patterned surface, the larger grit improved the TEG performance. For double-sided patterned TEGs, those with matched patterns (i.e., both surfaces formed from sandpaper with the same grit) demonstrated the highest performance.

Femtosecond laser direct writing is another useful tool for preparing micro- and nano-scale structures on different surfaces.[81] In a recent case using laser-writing, a PDMS (tribonegative) film was patterned with microbowl concave structures,[19] while the opposing side of the TEG was a copper (tribopositive) film with micro/nanocone convex structures. The dual-layer patterned TEG provided dramatically improved performance (0.21 W/m^2) relative to a single-layer patterned TEG (0.01 W/m^2).

The performance of TEGs generally improves with decreased feature size, increased feature density, and complimentary patterns on opposing surfaces. Following these guidelines, the real contact area between surfaces is maximized. Jang *et al.*[20] have proposed that the influence of micropatterning of PDMS films on triboelectric performance is only significant at high contact forces, where the elasticity of PDMS enables it to be completely deformed thus increasing the contact area between two surfaces. TEGs with pyramid-patterned PDMS as the negative triboelectric layer and silver (Ag) nanowires grown on an Al film as the positive triboelectric layer exhibited an ~6.7% decay in measured voltage after 30000 cycles of contact-separation motion under 2.5 kPa. Similarly, a sandpaper-cast PDMS-based TEG exhibited a 10% reduction in output voltage after 30 days of operation.[78]

Patterned TEGs can demonstrate limited performance in high humidity environments. As described in section 3.3.2, high environmental humidity can form a conductive water layer, thereby accelerating transition, neutralization, or dissipation of charges and inhibiting electrification of the material surface, whilst also potentially forming a shielding layer and inhibiting friction between the two solid surfaces.[82] Although PDMS is a relatively hydrophobic material, the patterns and features of these TEGs could lead to water being trapped during contact, resulting in charge screening and neutralization effects.

5.3. From Surface to Bulk Patterning

Surface modification via micro/nanostructuring, by nature, is sensitive to iterative frictional or contact-separation motion, which can wear away at the surface features. This degradation of surface features can be avoided by modifying the structure of the bulk material. A PDMS-based TEG with a 3-dimensional (3D) sponge-like structure (Figure 11(a)) has demonstrated an improved electric

performance relative to its flat counterpart (130 V and 50 V, respectively).[83] Interestingly, it appeared that the surface contact area did not play a major role in enhancing the performance, as the contact area of the 3D sponge-like PDMS was lower on the top surface compared to a flat PDMS sheet. Furthermore, the generated voltage of the sponge-like TEG increased with a decrease in pore size from 10 μm (68 V) to 0.5 μm (130 V), indicating the corresponding increase in the effective surface area of the pores affects the performance. The authors proposed that the enhanced energy harvesting performance was a result of charge generation through the surface of the inner pores by electrostatic induction. Notably, the reduced compressive modulus of the sponge-like PDMS TEG decreased the separation between the electrodes under compressive stress, thus increasing the capacitance and consequently leading to enhancements in energy harvesting performance.

Kim *et al.*[30] have created a similar 3D hierarchical structure by coating PDMS on sugar cubes and dissolving away the sugar templates following the curing of the PDMS. This templating resulted in a 10-fold enhancement in generated voltage (450 V) relative to a flat PDMS film (45 V) (Figure 11(b)). The authors also reported an increase in compression at equivalent force, despite the reduced contact area. This suggests that there may be material transfer within the pores that contributes to the energy harvesting performance, which is in line with the reports of radicals generated by compression of porous PDMS sponges.[84] The TEG with the smallest pore dimensions (i.e., smallest sugar cube template dimension, 300 μm) was reported to generate the highest voltage, attributed to the larger effective contact area. Moreover, the performance in a humid environment exhibited greater stability relative to the flat PDMS film, presumably due to the observed increase in hydrophobicity from the 3D hierarchical structure.

More recently, a hierarchical, sponge-like PDMS structure (Figure 11(c)) has been prepared by replica molding.[85] The mold consisted of a periodic grid up to two layers (20 μm grid separation for the first layer and 30 μm for the second layer) to form the surface structures. These multilayered structures resembled a step-pyramid. In order to induce porosity within the structures, one mold was coated with polystyrene particles (500 nm diameter) prior to PDMS curing. These polystyrene particles could be dissolved out to form a sponge-like internal structure. Going from a pillar (16 V), to a step-pyramid (20 V), and a porous step-pyramid (30 V) structure increased the energy harvesting performance.

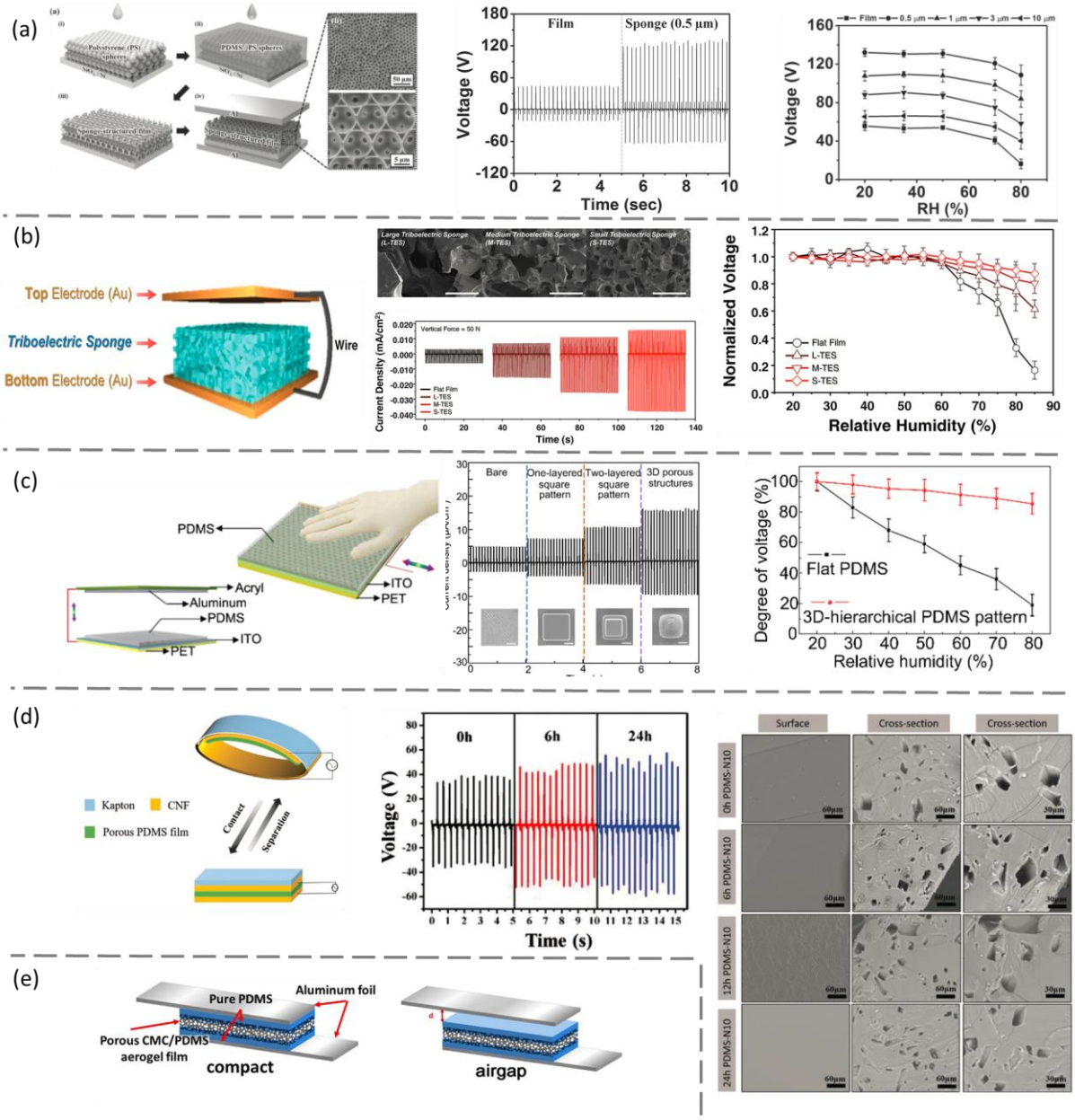

Figure 11. Electric output of sponge-structured PDMS TEGs. (a)-(c) Effect of porosity and relative humidity on electric output. (a) Comparison of the generated voltage between a film and sponge-like structure. Reproduced with permission.[83] Copyright 2014, WILEY-VCH. (b) Effect of the pore diameter on the generated current and voltage. Reproduced with permission.[30] Copyright 2016, WILEY-VCH. (c) Effect of surface structures on the generated current and voltage. Reproduced with permission.[85] Copyright 2019, Elsevier (d) Effects of the curing time on the generated voltage and morphology. Reproduced with permission.[86] Copyright 2020, WILEY-VCH. (e) Schematic demonstrating a new class of compact porous TEG, incorporating an air gap to eliminate surface friction-induced degradation. Reproduced with permission.[87] Copyright 2017, Elsevier.

A new self-assembly method has been developed for the generation of porous microstructures on PDMS films to eliminate the need to remove the pore-template. This method utilizes azobisisobutyronitrile (AIBN) as a blowing agent to control the architecture of the PDMS (Figure 11(d)).[86] The flat PDMS film showed internal porosity in the absence of surface porosity, enabling the direct comparison of surface contact area with non-porous films.

Although research has seldom focused on fundamental studies on the enhanced performance of 3D porous structures, beyond the stated increases in effective area and

capacitance, one potential mechanism has been proposed, based on the generation of mechano-radicals.[87] This has been undertaken by utilizing a porous carboxymethyl cellulose (CMC)/PDMS TEG. The PDMS was cast onto a freeze-dried CMC aerogel and subsequently coated with additional solid PDMS layers on the top and bottom surfaces to form the triboelectric layer (Figure 11(e)). The porous CMC/PDMS TEG exhibited a significantly higher generated voltage (17 V) relative to a CMC aerogel film TEG (negligible) or PDMS film TEG (5 V). The abundant cleavage of Si-O-Si bonds on PDMS and generation of radicals leads to the formation of transient dipole moments.[84] The majority of the newly formed radicals recombine, while a small fraction can react with trace water, forming silanols with a permanent electric dipole moment. Moreover, the rapid fluctuation in dipole moment during the formation and recombination of the mechano-radicals creates an electric potential between the two conformal electrodes. This potential enables the accumulation of charges and thus drives current flow. Hence, the authors proposed that the porous PDMS coating forms mechano-radicals under compression, in turn enhancing the energy harvesting performance. In this instance, the CMC aerogel provided a porous scaffold for the PDMS coating. This proposed effect was further confirmed by similar energy harvesting performance when substituting the CMC aerogel with alternative materials.[87]

In summary, 3D hierarchical structures have been shown to either maintain or improve the energy harvesting properties of TEGs with enhanced device durability relative to surface engineered solid films. Furthermore, 3D structures with porosity show reduced degradation in humid environments, in contrast to surface patterned TEGs. However, the underlying mechanism of the exceptional performance in 3D structured TEGs is yet to be established, with further detailed studies required.

5.4. Combined Materials and Structural Modification

With multiple strategies for performance enhancement being thoroughly explored, researchers have applied both structure and material modification simultaneously. However, as the complexity increases, various factors interplay, resulting in synergistic effects on performance enhancement. The added complexity makes it increasingly difficult to deconvolute the individual contributors of the performance enhancement.

For example, a flexible TEG, incorporating surface patterning and chemical functionalization has been reported.[88] The surface patterning was performed by coating PDMS onto a nickel– copper (Ni-Cu) textile, with an additional argon plasma treatment step. During the argon plasma step, tetrafluoromethane and oxygen gases are introduced into the chamber, resulting in chemical functionalization of the PDMS surface. An increase in performance (up to 100 V) was attributed to the fluorine treatment by increasing the electronegativity of the

PDMS surface. Conversely, the formation of nanostructured geometries was observed to hinder the energy harvesting performance due to a reduction in real contact area, in contradiction with previous studies.[21]

A nanowrinkle-patterned flexible woven TEG has been fabricated from a tribonegative PDMS/poly(vinylene difluoride) (PVDF) composite film and a tribopositive Ag foil.[89] The addition of PVDF was hypothesized to improve the dielectric properties, while maintaining the flexibility of the whole layer. Well-aligned wrinkle array architectures with a root-mean-square (RMS) roughness of 10 nm were produced after peeling off the cured blade-cast PDMS/PVDF film from the Al foil. The PVDF content simultaneously affected the dielectric permittivity, effective surface area and electron affinity of the PDMS/PVDF layer, consequently influencing the TEG performance. The optimal performance was obtained at 6 wt% PVDF, with a thickness of 2 mm. The resultant optimized TEG exhibited an open-circuit voltage of 255 V, current of 22 μA and power density of 832 mW/m^2.

Finally, a PDMS TEG has been fabricated by spraying the PDMS onto a Cu-nanowire decorated Cu mesh in order to create a roughened PDMS surface. This resulted technique in a four-fold enhancement in the open-circuit voltage (155 V) relative to PDMS sprayed onto a flat Cu film (38 V).[90]

5.5. Relating Performance to the Contact Electrification Mechanism

The literature for PDMS-based TEGs primarily assumes electron transfer as the default mechanism for TE. However, the majority of fundamental studies on the electron transfer mechanism for CE or TE focus on the metal/silica material pair rather than the polymer pair. The field is further complicated by the lack of a general model for the prediction of TEG performance, as the performance can be influenced by a number of contributing factors. Recent work has begun modelling the performance of TEGs using theoretical calculations based on the electron transfer mechanism, where the electronic structure of polymers is represented by molecular orbitals and chain alignment. Following the recent advances in experimental studies discussed throughout this review, the integration of the effects of contact area and force into theoretical models is emerging in literature.

Vasandani *et al.*[9] have theoretically derived a linear relationship between the applied contact force and the resultant triboelectric charge using fixed triboelectric material pairs. They reported an inverse proportionality between the generated surface charge and the critical separation distance between the material pairs. The model was compared to experimental results for a PET/PDMS TEG (Figure 12(a)). The error, however, between the predicted and experimental results was nearly five-fold. Thus, this model (which only considered electron transferred) failed to accurately predict the performance indicating that the process is not only driven by electron

transfer, or at least the electron transfer is enhanced by complimentary mechanisms. [9]

Wu *et al.*[91] have used first-principles calculations to challenge the most commonly proposed strategy (increasing the real contact area) to achieve improved performance in TEGs. They proposed that TEG performance can be enhanced by increasing the stress in the contact region, rather than only increasing in the real contact area. They investigated the metal-polymer CE mechanism using first-principles on an Al-PTFE triboelectric pair as a model. The contact state was deduced from the total energy at the interface with varying separation between the two layers, obtaining an equilibrium separation at 2.25 Å. Subsequently, the charge transfer correlated to the calculated separation-dependent Mulliken charge populations. The results showed an increase in charge transfer as the compression increased (i.e., a decrease in interface separation and increase in stress). Importantly, this study has also revealed that charge transfer can occur without contact at separation distances up to 5 Å (Figure 12(b)). The generation of electron-deficient structures under friction significantly lowers the LUMO at the interface and consequently increases the amount of electron transfer, in agreement with previous experimental studies on the role of mechano-ions and mechano-radicals in TE.[66]

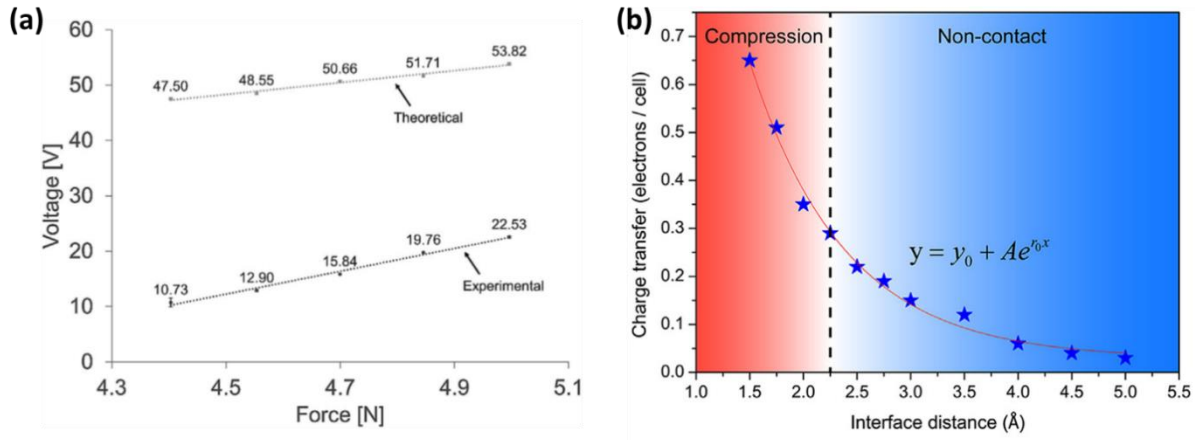

Figure 12. (a) Comparison of the theoretical prediction and experimental data for the dependence of open-circuit voltages of a TEG on the input force. Reproduced with permission[9]. Copyright 2017, Elsevier. (b) The calculated amounts of charge transfer at the interface distance between 1.5 Å and 5.0 Å. Reproduced with permission[91]. Copyright 2018, Elsevier.

For surface patterned TEGs, the cross-linking degree of PDMS, which is directly linked to elastic modulus, influences the extent of bond cleavage during contact-separation. The effect of elastic modulus on the TE has recently been studied by multiple groups. Pandey *et al.*[18, 49] have studied the material transfer mechanism, correlating the elastic modulus with the cohesive energy of the material. The authors have observed an improvement in the energy harvesting performance by lowering the modulus of one surface of PDMS. The lower cohesive energy of softer material promotes the transfer of charged segments, directly correlating with the observed enhancement in energy

harvesting performance (Figure 13, (a)). However, a contrasting result is obtained by Kim *et al.*[19], finding a reduction in energy harvesting performance for PDMS with lower modulus (Figure 13, (b)). This finding is justified by the relative ease of reducing surface roughness with an applied pressure for PDMS with a reduced modulus, thus reducing the electron transfer. It is clear that the change in modulus does not only modify the degree of deformation, affecting the real contact area, but also alters the cohesive energy, affecting the ability of PDMS to cleave bonds in material transfer.

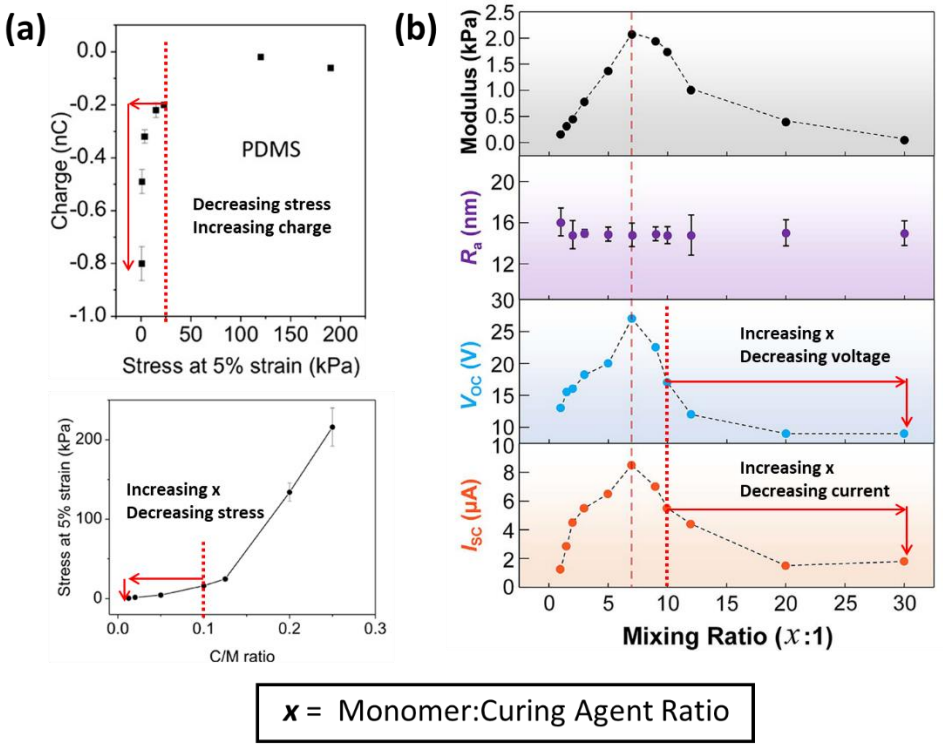

Figure 13. Correlation between the monomer to curing agent ratio (x: 1) and electrical output of the TEG. To compare the same range x > 10, (a) electric performance increases as x increases. Adapted with permission.[18] Copyright 2018, American Chemical Society.; (b) electric performance decreases as x increases. Adapted with permission [19]. Copyright 2017, Elsevier.

Overall, there is little doubt that PDMS is an ideal material to study CE and TE, with flexibility in mechanical properties, surface patterning, bulk modification, and additives enabling a clear understanding of fundamental mechanisms to be developed. However, despite the power and flexibility of PDMS as a triboelectric material, conflicting results remain. Many reports are focused on a single mechanism or modification approach, without tying past understanding together. The following section summarizes and combines the concepts discussed above, providing a perspective for the field moving forward.

6. Summary and Outlook

6.1. Contact Electrification Mechanism: Electron, Ion, and Material Transfer

In general, when two triboelectric layers are brought into contact charges are transferred, and after the two layers are separated, a potential difference is generated

which can be measured or used externally. Macroscopically, the two layers are brought into contact and reach the final compressed position, whilst microscopically the local separation between the two surfaces can span multiple orders of magnitude, between μm and Å. This microscopic separation is considered to be in 'real contact' provided it falls within the separation range where electron transfer, ion transfer, or material transfer can occur, as shown in Figure 14 using the Lenard-Jones Potential curves, and summarized in Table 3.[92] This means all three types of charge carriers can be transferred between materials, and indeed the dominance of the charge carrier type can be tuned for equivalent materials by changing the interfacial matching and applied force.

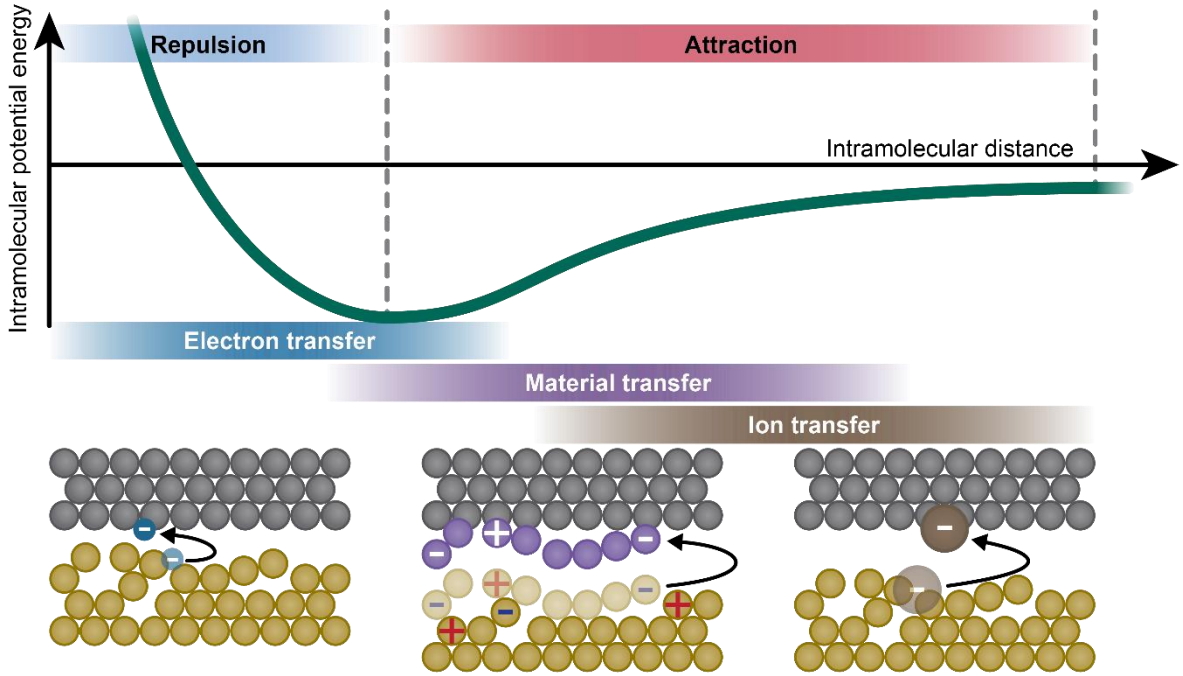

Figure 14. Conceptual representation of the Lenard-Jones Potential curve demonstrating the real contact state (energy regime where transfer can occur) for electron, ion, and material transfer mechanisms. The real contact state of the electron transfer mechanism falls in the repulsive region, whereas the ion transfer and material transfer mechanism fall in the attraction region.[91, 93]

Unlike the material transfer mechanism, the electron transfer mechanism and ion transfer mechanism have been more thoroughly studied, with a general agreement on the CE process reached. For triboelectric pairs without built-in mobile ions, the ion transfer mechanism is generally agreed to be a direct result of water in the atmosphere adsorbing on both surfaces of the TEG and transferring across during contact, enabled by the differences in the binding energy of the respective surfaces.

Table 3. Requirements for different contact electrification mechanisms.

Charge Carrier	Distance/Force Range	Additional Condition for Charge Transfer
Electron	When electron clouds overlap (repulsive region)	The energy barrier has been eliminated for electrons to transfer from HOMO state of one material to LUMO state of the other material.
Ion	When exerting ion-dipole forces OR ion-induced-dipole forces	There are environmental ions able to be adsorbed on the material, gas molecules able to be ionised, or existing mobile ions within or on the polymer surface. The binding energy of ion to the other material is larger than its adsorption force to its current binding material.
Material	When exerting adhesion[93]	The adhesion energy between the material surfaces is larger than the cohesion energy of either material.

Understanding the driving force for electron transfer in CE between two dielectric materials is a focus of ongoing research with models being proposed and adapted to explain the process.[53, 54, 94, 95] The potential-well model explains the role of large stress and small distance on lowering the energy barrier for electron transfer in CE, which is also used to explain the effects of temperature,[53] surface curvature and light-irradiation on CE.[94] Theoretically, all factors which affect the energy difference between the HOMO and LUMO states of the two materials can, in principle, affect the electron transfer process. However, for metal-polymer pairs, a first-principles calculation has concluded that electron transfer can occur outside the repulsive force regime,[91, 96] conflicting with the experimental results of Wang *et al.* on metal-silica pairs.[97-99] For polymer-polymer pairs, an early study suggests electron transfer in polymer-polymer CE is enabled by the formation of mechano-particles[66] and more recent studies have directed their focus to probing the role of material transfer in TE.[18, 61, 65]

It is commonly agreed that material transfer occurs when the distance between two materials is in the attractive regime, where segments of the material with a lower cohesion energy will be fragmented due to covalent bond cleavage, creating mechano-radicals and mechano-ions. Material transfer or bond cleavage have been demonstrated to correlate to triboelectric charging for systems consisting of metal-polymer,[67] polymer-polymer[18] and even identical polymer pairs,[61] and are more often reported to be related to soft and porous materials.[18, 87] The generation of these mechano-radicals, mechano-anions and mechano-cations is generally believed to be the cause of the mosaic charge patterns after repeated TE cycling.[65] However, these studies have only provided half of the picture, only showing how material transfer/bond cleavage initiates TE. It is still unclear how the transfer of

charged material segments results in the net charge between the two layers. In the authors' view, the following three events impact the TE through material transfer, either directly or indirectly:

1. Heterolytic bond cleavage creates mechano-particles that form the mosaic charge pattern.
2. Mechano-particles are subsequently brought into further close contact during contact-separation cycling leading to redox reactions at the material interface, or transfer between surfaces thus reversing the local charge.
3. The mechano-radicals formed in the first event react with the environment, terminating further reactions.

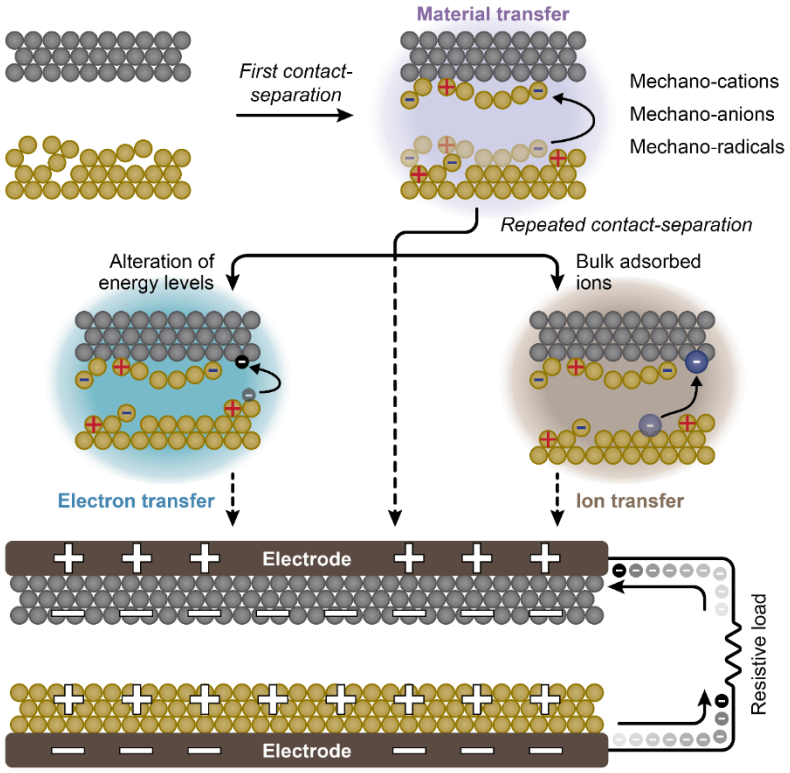

Figure 15. Schematic demonstrating the role of material transfer in secondary ion transfer and electron transfer. Material transfer leads directly to the formation of mechano-cations/anions/radicals, which could further act as bulk ions charging the surfaces by ion transfer, or alter the energy states of electrons promoting charging by electron transfer.

The first contact-separation event is the starting point of TE by material transfer, with induced mechano-radicals and mechano-ions formed on the surface of each material. The second event can be either electron transfer, initiated from the change in electronic structure induced by these charged fragments, or ion transfer from adsorbed water to compensate the charge of the fragments. As there is no clear driving force for continued charge separation, subsequent events can cancel out or reverse the sign of the charge generated during the first contact-

separation event. Therefore, the material transfer mechanism is a competition between the formation of mechano-particles due to material transfer, bulk mechano-ion transfer, electron transfer across mechano-particles and the termination of radicals (Figure 15). Crucially, the role of material transfer in influencing electron and ion transfer mechanisms is rarely discussed in literature, leading to the ambiguous and conflicting results when one mechanism is omitted.

The debate on which CE mechanism is dominant in any given material combination is ongoing. However, most research groups that study the electron transfer mechanism focus on metal-dielectric pairs, and those who study the ion/material transfer mechanism focus on dielectric-dielectric pairs. Realizing this, a recent study suggests the dominant mechanism depends on the triboelectric pair.[68] Nevertheless, a better approach might be to focus on how different charge transfer processes interplay with each other under different conditions, instead of attempting to demonstrate a single dominant mechanism for all instances.

6.2. Triboelectricity in energy generators: More than just contact electrification

In the context of TEGs, it is more appropriate to refer to CE as TE to extend the length scale from the molecular level to a macroscopic level. In this case, when a contact force is applied to bring two materials into contact, an elastic material will deform, inducing horizontal relative motion and friction between the two materials. Triboelectric charging by different mechanisms in localized regions of the same sample will then emerge upon removal of the contact force, provided the additional conditions in Figure 14 are satisfied. If one or both triboelectric layers are porous, the compressed sponge-like structure will lead to a more significant decrease in separation between two electrodes and the generation of more mechano-particles.[84] Both of these factors will affect the electrical performance of the TEG

The above processes only consider the TE between two solid surfaces. However, water can also play a role, thereby complicating the process. The water layer formed due to a highly humid atmosphere can shield charges, leading to decreases in performance in humid environments. However, water can also transfer electrons to the solid surface and provide a source of ions for ion transfer during TE, leaving the transferred electrons or/and adsorbed ions on the solid surface once the water is removed. Moreover, the two charged surfaces can lead to the formation of either an electrical double layer at the material-water interface[71] or ionized air upon rapid motion and close contact.[58] In both cases, the surface charges on the triboelectric surfaces will be screened and vary dynamically during the contact-separation process.

6.3. Performance enhancement of triboelectric energy generators

Since the emergence of TEGs, the morphology of the contacting surfaces has been tailored to increase the real

contact area, which has often directly led to improved electrical output. However, the phrase used in most papers, "real contact area", is an intuitive concept which generally represents the contact area between two surfaces which allows for charge transfer to take place. In most instances, this is considered to be the contact area specifically for electron transport. Understanding what constitutes the 'real contact' area is challenging as it varies between the two contacting materials and is driven by the different force regimes in which the charge transfer mechanisms occur.

Recent work has shown that it is more effective to increase the local stress exerted on the contacting surfaces, as opposed to striving for a continued increase in contact area.[91] Multiple studies have demonstrated that the stress experienced during TE is increased by using micro/nano-patterns with a higher ability to deform.[20, 22, 76, 78] This increased stress changes the electronic structure of the material and decreases the separation required (lowers the activation energy) for a given charge transfer mechanism, thus effectively increasing the real contact area. Thus, considering ways to increase the real contact area remains crucial, however the field should consider the role of deformation and stresses on the surface of the material as a mechanism to increase the contact area.

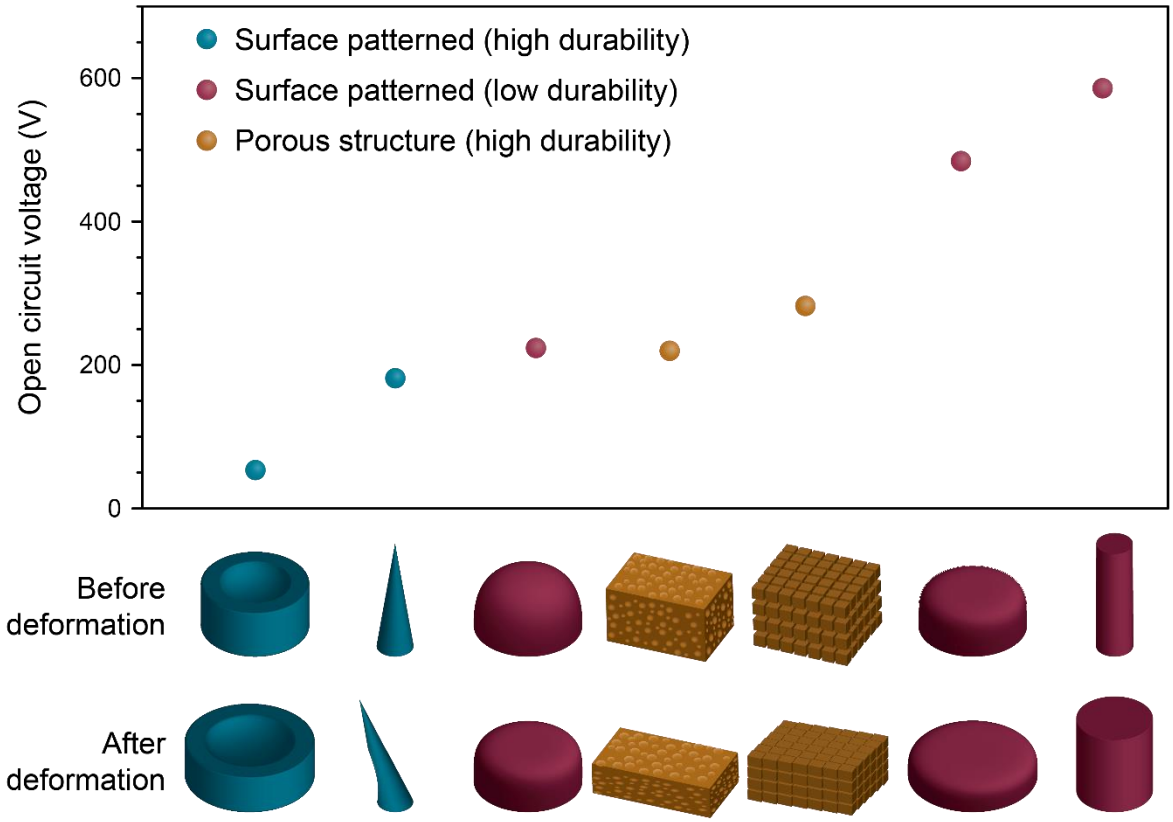

Figure 16. Representative data highlighting the effect of structure on electrical performance of TEGs. Data obtained from references (a)[19](b)[76](c)[20](d)[85](e)[30](f)[22](g)[21].

However, while the electrical performance can be improved by an increase in stress on the contact region, the increased stress can ultimately lead to degradation, thus reducing the durability of the TEGs (Figure 16). For instance, convex-shaped and micro/nanoscale patterns[20-22] can generate improved energy harvesting performance relative to flat, concave-shaped[19] or millimeter scale patterns;[76, 80, 100] however, such patterns experience accelerated performance degradation over time. To balance the maximum energy harvesting performance and the durability of the TEGs, one emerging approach is to fabricate 3D sponge-like structures.[30, 85] These 3D sponge-like structures can maintain high energy harvesting performance and ensures durability due to a more homogenous distribution of stress throughout the sponge-like material.

Recently, more studies have investigated the performance of sponge-like PDMS TEGs. It is clear from these reports that the porosity of the sponge-like TEGs is the dominant factor affecting the performance (having a larger effect than changing the contact surface area).[30, 85] As summarized in section 5.3, the operational principle of sponge-like TEGs is complex, involving multiple processes which interplay and affect the overall performance. Specifically, material transfer within pores is exceptionally hard to isolate, but is likely to play a major role in the enhancement of charge generation. Systematic studies are required to improve the understanding of sponge-like structures. The proposed reasons for increases in energy harvesting performance are listed below:

1. generation of mechano-radicals in pores under stress;[87]
2. low required force required for a large of compressive deformation; and
3. increased friction between contact surfaces due to large volumetric deformation.

The reduction in durability of TEGs is another case where empirical data trumps a clear understanding. The reasons for the degradation of TEGs vary upon the system being studied, however the potential reasons include:

1. physical degradation of the surface morphology acting to reduce real contact area;
2. continuous material transfer and surface fragmentation forming a shielding layer, reducing surface charge density or polarity reversal;[49] or
3. reaction of stress-generated mechano-radicals with the atmosphere[87] changing the surface chemical composition.

In general, the optimal structure of a TEG is application dependent. Sensors aiming for high sensitivity require meticulously designed architectures of surface patterns, in turn allowing a gradual increase in contact area under stress. Alternatively, 3D sponge-like structures are optimal if a high peak electrical output is targeted. Exceptional reports detailing engineering and application advances for PDMS (and polymer) TEGs can further elaborate on these structural and device specific modifications.[101, 102]

An improved understanding of CE is necessary for continued engineering enhancement of TEGs. Currently,

electron transfer is the default mechanism used to explain the electrical performance of TEGs and the material transfer mechanism is sparsely discussed. To efficiently move forward in engineering high performance TEGs, we propose studies should focus on fundamentally understanding the following questions:

How can electron, ion, and material transfer mechanisms be understood in a single system, over multiple contact-separation cycles?

1. What explains the exceptional performance of sponge-like TEGs?
2. What information can be interpreted from the shape of V_{oc}/I_{oc} signals?
3. How can electrical performance be predicted using theoretical calculations?
4. By answering these questions, the conflicting literature reports and theories can be re-examined and codified in a clear model explaining how to control and optimize the properties of TEGs.

6.4. Energy Generators to Study Contact Electrification

TEGs have not only been utilized as a device for multiple applications, they have also often been used as a tool for fundamental CE studies. The direct result of CE is the separation of surface charge density distributed on the two triboelectric layers, which is related to the voltage/current generated. Therefore, by simply comparing the stress-induced generation of voltage/current, the CE mechanism can be studied under different conditions. However, the reality is more complicated, considering differing results can be observed by tuning the same parameters of a TEG. This mismatch in experimental results arises due to the interplay of multiple factors (Figure 17). Hence, meticulous and methodical experimental design is critical to generate reliable results. The experimental design must be paired with careful analysis when considering the interplaying factors. Most importantly, the experimental design should aim to take into consideration all three CE mechanisms, rather than selectively choose one mechanism to explain the observed phenomena.

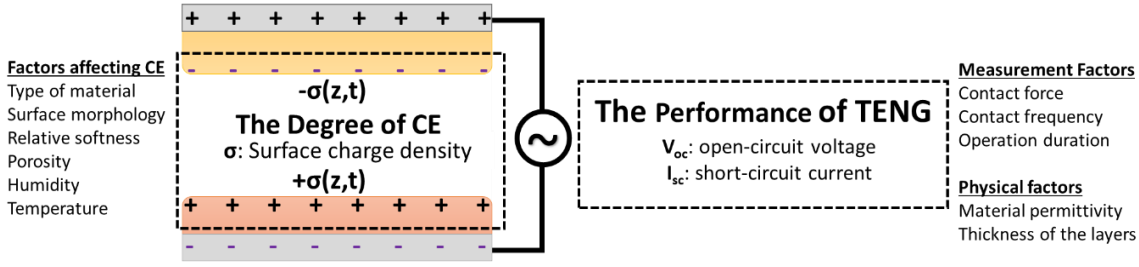

Figure 17. Factors affecting the degree of contact electrification and the electrical performance of a TEG.

Though using TEGs to study CE can be convenient, limitations remain, which hinder the extraction of information from the generated voltage/current as the only evidence. For instance, the V_{oc}/I_{sc} can only give information on the net surface charge and the polarity of the two triboelectric surfaces. However, the previously verified mosaic charge pattern, which strongly correlates to material transfer, cannot be detected. Therefore, it is necessary to combine other characterization methods to extract more information from TEGs for the elucidation of CE mechanisms. Moreover, the information from output voltage and current signals have not been completely utilized for CE analysis in most studies except for the peak values. The shape of the output voltage/current signals (e.g., the inherent asymmetric nature of current output[103]) correlating to the contact-separation motion at various measuring conditions can give insights into the CE mechanism.

6.5. A comment on measurement and reporting

The measurement of triboelectric phenomena, and the reporting of record currents, voltages, charges, and powers has exploded in recent years. It is important for readers to critically analyze the data presenting in literature, as there is often confusion surrounding the source of electrical energy generation. In the case of polymer triboelectric materials, there is the possibility for either thermal energy generation from the pyroelectric effect or mechanical energy conversion from the piezoelectric effect[104] to be mistaken for triboelectric devices.[105] The electrical waveforms generated by these related techniques is so similar that it is near impossible to deconvolute. Indeed, it has recently been reported that hybrid piezo-triboelectric devices enhance the energy generation by both mechanisms. Indeed, recent works by Ahmed et al.,[106] and Sutka et al.,[104] have provided strong commentary examining this enhancement by contrasting and deconvoluting the piezoelectric and triboelectric effects. While, there have been no discussion papers on confusion between pyroelectric and triboelectric outputs, it is logical that the friction at the interface leads to localised heating and a temperature gradient that could induce some current or charge flow.[107, 108] The synergy between these effects is highlighted by the emergence of hybrid energy harvesting devices based on combined piezo-pyro-triboelectric effects.[109]

A further challenge in ascertaining and ascribing generated electrical outputs to the triboelectric effect is deconvolution from the flexoelectric effect. The flexoelectric effect is simply the property of a material to generate electrical charge from a strain gradient.[110] In pure CE studies, which examine a vertical contact-separation motion, there should be negligible strain gradients induced. The flexoelectric voltage output of ∓ 1 to 10 V, as modelled by Mizzi, Lin and Marks[111] during simple contact separation, demonstrates the significant contribution that flexoelectricity can have. Introducing tortuous porosity, nanostructure and surface topography (all approaches to improve triboelectric real-contact area) can lead to significant charge output from the flexoelectric effect.[112-114] This is further complicated by the lack of detailed infor-

mation on flexoelectric coefficients for common polymers, and is a field that merits further study. Thus, while exploitation of the flexoelectric effect is beneficial for energy harvesting applications, its contributions must be considered when dramatically changing the morphology of triboelectric energy generators.[111]

The field of polymer and PDMS triboelectric energy harvesting is exceptionally exciting, it is crucial authors carefully review their device performance and provide key experimental parameters so a clear vision of the field is possible.

6.6. What about the triboelectric series?

The triboelectric series has long been used as an approximation of CE between two different materials. However, the rationality of using the triboelectric series as a tool for CE should be challenged. Firstly, its format, the ordering of materials with differing chemical structures, establishes a first fundamental belief that the key to the difference in CE originates from the difference in chemical structure. However, CE between identical materials has been demonstrated, showing that CE can be due to random fluctuations at the molecular scale which cannot be represented by a single averaged material property derived from its bulk chemical structure.[48, 49]

Secondly, the common attempt of rationalizing the ordering of a triboelectric series using a specific material property to argue a dominant mechanism, establishes a fundamental belief that there is a universal CE mechanism. However, the literature discussed in this review regarding the impact of a single property on multiple mechanisms suggests the absence of a universal CE mechanism which can be strictly represented by a single material property.

Nevertheless, there remain studies[56, 66] which rationalize the triboelectric series from extrapolation of a single material property and conclude that the CE mechanism related to that property is dominant. However, while these present only half the picture of CE, it is reckless to totally repudiate their arguments. The fact that triboelectric series are often non-reproducible in different measurement methods, combined with the above summary on the intricacies of the CE process, demonstrates that the ordering of the triboelectric series can be "selected" by the experimental technique, focused on a specific mechanism.

Hence, while the argument for a universal dominant CE mechanism presents an incomplete view of the field, it is important to draw value from these statements. Upon realizing the measurement and environmental dependence of CE, it is rational to argue that these broad statements around a single dominant mechanism arise from a focus on specific material properties (as exemplified by PDMS) that are most influenced by that mechanism. This understanding enables clarity of how to quantitatively compare and use the variety of excellent research on triboelectric series in practical TEGs.

7. Conclusions

In conclusion, the research on PDMS TEGs is predominantly empirical and a thorough understanding of how variations in surface, bulk, and chemical properties interplay with fundamental CE mechanisms is crucial. PDMS is an ideal material to study CE and enables exceptional TEG performance, due to its chemical and physical tuneability coupled to its propensity for heterolytic bond cleavage. However, studies on how the on the effects of crosslinking density impact the performance of PDMS TEGs has yielded contradictory results in different studies. Different positive materials can be used to study the influence of adhesion force, whilst the surface morphology, thickness and testing conditions (applied stress and frequency) are paramount to study the influence of any given parameter on the electric performance of the TEG.

Performance enhancement is often explained by increasing the real contact area between layers, with charge formation attributed to electron transfer, whilst material transfer has been largely overlooked. For surface-patterned PDMS-TEGs, the increase in both the stress at the contact region and the degree of deformation have been revealed to play a significant role in performance enhancement. For sponge-structured PDMS TEGs, the performance enhancement has not been thoroughly explained and related to CE mechanisms. However, the significant role of the formation of mechano-particles in the sponges has recently emerged.

To understand CE and TEG performance, the complexity of interactions material transfer, electron transfer, and ion transfer mechanisms requires further study. Fundamental studies need to be designed with great care due to the complexity and environmental sensitivity of CE. The triboelectric series can be used as a tool for CE studies, but the experimental conditions must be meticulously designed, and limitations clearly stated such that specific properties of a material can be tied to specific charge transfer mechanisms.

Within this review we have posed questions critical to advancing the field of polymer triboelectric materials, which requires a thorough understanding of flexoelectric, piezoelectric and triboelectric mechanisms. Moving forward, multidisciplinary teams with skills in materials chemistry, physics, engineering, and computational modelling will be required to form a holistic answer to these questions. Focusing on describing complex triboelectric effects from the perspective of a single research field cannot capture the breath and disparate factors that drive contact electrification and the triboelectric effect. Fundamental contact electrification studies can boost their accuracy by including finite element modelling of strain fields to exclude the flexoelectric effect, molecular dynamics or density functional theory calculations to understand material transfer, and humidity-controlled experiments to elucidate the role of water and/or ion transfer within the system. In the case of applied triboelectric

generator literature, it is important to highlight the potential role of alternate mechanical-to-electrical conversion mechanisms (including piezo-, pyro-, and flexo-electric effects, and ion and mass transfer) within the data. Indeed, these complexities mean that in many cases it is preferable to either term a triboelectric energy harvester as a hybrid system or discuss mechanical-to-electrical conversion performance when detailed mechanistic studies are not included in the original research article.

Triboelectric energy harvesting is an exceptionally exciting field. Through understanding the mechanisms that lead to reported device performances, new paradigms of device design and energy conversion efficiency will be achieved.

References

1. Henniker, J., Triboelectricity in Polymers. *Nature* **1962,** 196, (4853), 474-474.
2. Lacks, D. J.; Shinbrot, T., Long-standing and unresolved issues in triboelectric charging. *Nature Reviews Chemistry* **2019,** 3, (8), 465-476.
3. Seol, M.; Kim, S.; Cho, Y.; Byun, K. E.; Kim, H.; Kim, J.; Kim, S. K.; Kim, S. W.; Shin, H. J.; Park, S., Triboelectric Series of 2D Layered Materials. *Advanced Materials* **2018,** 30, (39), e1801210.
4. Diaz, A. F.; Felix-Navarro, R. M., A semi-quantitative tribo-electric series for polymeric materials: the influence of chemical structure and properties. *Journal of Electrostatics* **2004,** 62, (4), 277-290.
5. Coehn, A., Ueber ein Gesetz der Electricitätserregung. *Annalen der Physik* **1898,** 300, (2), 217-232.
6. Hersh, S. P.; Montgomery, D. J., Static Electrification of Filaments:Experimental Techniques and Results. *Textile Research Journal* **1955,** 25, (4), 279-295.
7. Adams, C. K., *Nature's electricity*. Tab Books: Blue Ridge Summit, PA, 1987, pg 63.
8. Fan, F. R.; Lin, L.; Zhu, G.; Wu, W.; Zhang, R.; Wang, Z. L., Transparent triboelectric nanogenerators and self-powered pressure sensors based on micropatterned plastic films. *Nano Letters* **2012,** 12, (6), 3109-14.
9. Vasandani, P.; Mao, Z.-H.; Jia, W.; Sun, M., Relationship between triboelectric charge and contact force for two triboelectric layers. *Journal of Electrostatics* **2017,** 90, 147-152.
10. Nguyen, V.; Yang, R., Effect of humidity and pressure on the triboelectric nanogenerator. *Nano Energy* **2013,** 2, (5), 604-608.
11. Xu, C.; Wang, A. C.; Zou, H.; Zhang, B.; Zhang, C.; Zi, Y.; Pan, L.; Wang, P.; Feng, P.; Lin, Z.; Wang, Z. L., Raising the Working Temperature of a Triboelectric Nanogenerator by Quenching Down Electron Thermionic Emission in Contact-Electrification. *Advanced Materials* **2018,** 30, (38), e1803968.
12. Wang, Z. L., Triboelectric Nanogenerator (TENG)—Sparking an Energy and Sensor Revolution. *Advanced Energy Materials* **2020,** 10, (17).
13. Hillborg, H.; Gedde, U. W., Hydrophobicity recovery of polydimethylsiloxane after exposure to corona discharges. *Polymer* **1998,** 39, (10), 1991-1998.
14. Mark, J. E., Some Interesting Things about Polysiloxanes. *Accounts of Chemical Research* **2004,** 37, (12), 946-953.
15. Zaman, Q.; Zia, K. M.; Zuber, M.; Mabkhot, Y. N.; Almalki, F.; Hadda, T. B., A comprehensive review on synthesis, characterization, and applications of polydimethylsiloxane and copolymers. *International Journal of Plastics Technology* **2019,** 23, (2), 261-282.
16. Mazur, T.; Grzybowski, B. A., Theoretical basis for the stabilization of charges by radicals on electrified polymers. *Chemical Science* **2017,** 8, (3), 2025-2032.
17. Menhofer, H.; Heusinger, H., Radical formation in polydimethylsiloxanes and polydimethyldiphenylsiloxanes studied by the ESR spintrap technique. *International Journal of Radiation Applications and Instrumentation. Part C. Radiation Physics and Chemistry* **1987,** 29, (4), 243-251.
18. Pandey, R. K.; Kakehashi, H.; Nakanishi, H.; Soh, S., Correlating Material Transfer and Charge Transfer in Contact Electrification. *The Journal of Physical Chemistry C* **2018,** 122, (28), 16154-16160.
19. Kim, D.; Tcho, I.-W.; Jin, I. K.; Park, S.-J.; Jeon, S.-B.; Kim, W.-G.; Cho, H.-S.; Lee, H.-S.; Jeoung, S. C.; Choi, Y.-K., Direct-laser-patterned friction layer for the output enhancement of a triboelectric nanogenerator. *Nano Energy* **2017,** 35, 379-386.
20. Jang, D.; Kim, Y.; Kim, T. Y.; Koh, K.; Jeong, U.; Cho, J., Force-assembled triboelectric nanogenerator with high-humidity-resistant electricity generation using hierarchical surface morphology. *Nano Energy* **2016,** 20, 283-293.
21. Dudem, B.; Huynh, N. D.; Kim, W.; Kim, D. H.; Hwang, H. J.; Choi, D.; Yu, J. S., Nanopillar-array architectured PDMS-based triboelectric nanogenerator integrated with a windmill model for effective wind energy harvesting. *Nano Energy* **2017,** 42, 269-281.
22. Bui, V. T.; Zhou, Q.; Kim, J. N.; Oh, J. H.; Han, K. W.; Choi, H. S.; Kim, S. W.; Oh, I. K., Treefrog Toe Pad-

Inspired Micropatterning for High-Power Triboelectric Nanogenerator. *Advanced Functional Materials* **2019,** 29, (28).
23. Kim, D.; Lee, S.; Ko, Y.; Kwon, C. H.; Cho, J., Layer-by-layer assembly-induced triboelectric nanogenerators with high and stable electric outputs in humid environments. *Nano Energy* **2018,** 44, 228-239.
24. Qian, C.; Li, L.; Gao, M.; Yang, H.; Cai, Z.; Chen, B.; Xiang, Z.; Zhang, Z.; Song, Y., All-printed 3D hierarchically structured cellulose aerogel based triboelectric nanogenerator for multi-functional sensors. *Nano Energy* **2019,** 63.
25. Wolf, M. P.; Salieb-Beugelaar, G. B.; Hunziker, P., PDMS with designer functionalities—Properties, modifications strategies, and applications. *Progress in Polymer Science* **2018,** 83, 97-134.
26. Zhu, D.; Handschuh-Wang, S.; Zhou, X., Recent progress in fabrication and application of polydimethylsiloxane sponges. *Journal of Materials Chemistry A* **2017,** 5, (32), 16467-16497.
27. Venkatachalam, S.; Hourlier, D., Heat treatment of commercial Polydimethylsiloxane PDMS precursors: Part I. Towards conversion of patternable soft gels into hard ceramics. *Ceramics International* **2019,** 45, (5), 6255-6262.
28. Chen, Z.; Khajeh, A.; Martini, A.; Kim, S. H., Chemical and physical origins of friction on surfaces with atomic steps. *Science Advances* **2019,** 5, (8), eaaw0513.
29. Niu, S.; Wang, S.; Lin, L.; Liu, Y.; Zhou, Y. S.; Hu, Y.; Wang, Z. L., Theoretical study of contact-mode triboelectric nanogenerators as an effective power source. *Energy & Environmental Science* **2013,** 6, (12).
30. Kim, D.; Park, S.-J.; Jeon, S.-B.; Seol, M.-L.; Choi, Y.-K., A Triboelectric Sponge Fabricated from a Cube Sugar Template by 3D Soft Lithography for Superhydrophobicity and Elasticity. *Advanced Electronic Materials* **2016,** 2, (4).
31. Zhu, G.; Pan, C.; Guo, W.; Chen, C. Y.; Zhou, Y.; Yu, R.; Wang, Z. L., Triboelectric-generator-driven pulse electrodeposition for micropatterning. *Nano Letters* **2012,** 12, (9), 4960-5.
32. Chen, L.; Shi, Q.; Sun, Y.; Nguyen, T.; Lee, C.; Soh, S., Controlling Surface Charge Generated by Contact Electrification: Strategies and Applications. *Advanced Materials* **2018,** 30, (47), e1802405.
33. Zhang, X.; Lv, S.; Lu, X.; Yu, H.; Huang, T.; Zhang, Q.; Zhu, M., Synergistic enhancement of coaxial nanofiber-based triboelectric nanogenerator through dielectric and dispersity modulation. *Nano Energy* **2020,** 75.
34. Wen, R.; Guo, J.; Yu, A.; Zhai, J.; Wang, Z. l., Humidity-Resistive Triboelectric Nanogenerator Fabricated Using Metal Organic Framework Composite. *Advanced Functional Materials* **2019,** 29, (20).
35. Jing, T.; Xu, B.; Yang, Y., Liquid doping materials as micro-carrier of functional molecules for functionalization of triboelectric materials and flexible triboelectric nanogenerators for energy harvesting and gesture detection. *Nano Energy* **2020,** 74.
36. Li, G. Z.; Wang, G. G.; Ye, D. M.; Zhang, X. W.; Lin, Z. Q.; Zhou, H. L.; Li, F.; Wang, B. L.; Han, J. C., High-Performance Transparent and Flexible Triboelectric Nanogenerators Based on PDMS-PTFE Composite Films. *Advanced Electronic Materials* **2019,** 5, (4).
37. Li, Z. B.; Li, H. Y.; Fan, Y. J.; Liu, L.; Chen, Y. H.; Zhang, C.; Zhu, G., Small-Sized, Lightweight, and Flexible Triboelectric Nanogenerator Enhanced by PTFE/PDMS Nanocomposite Electret. *ACS Applied Materials Interfaces* **2019,** 11, (22), 20370-20377.
38. Kim, D. W.; Lee, J. H.; Kim, J. K.; Jeong, U., Material aspects of triboelectric energy generation and sensors. *NPG Asia Materials* **2020,** 12, (1).
39. Song, G.; Kim, Y.; Yu, S.; Kim, M.-O.; Park, S.-H.; Cho, S. M.; Velusamy, D. B.; Cho, S. H.; Kim, K. L.; Kim, J.; Kim, E.; Park, C., Molecularly Engineered Surface Triboelectric Nanogenerator by Self-Assembled Monolayers (METS). *Chemistry of Materials* **2015,** 27, (13), 4749-4755.
40. Feng, S.; Zhang, H.; He, D.; Xu, Y.; Zhang, A.; Liu, Y.; Bai, J., Synergistic Effects of BaTiO3/Multiwall Carbon Nanotube as Fillers on the Electrical Performance of Triboelectric Nanogenerator Based on Polydimethylsiloxane Composite Films. *Energy Technology* **2019,** 7, (6), 1900101.
41. Lapčinskis, L.; Linarts, A.; Mālnieks, K.; Kim, H.; Rubenis, K.; Pudzs, K.; Smits, K.; Kovaļovs, A.; Kalniņš, K.; Tamm, A.; Jeong, C. K.; Šutka, A., Triboelectrification of nanocomposites using identical polymer matrixes with different concentrations of nanoparticle fillers. *Journal of Materials Chemistry A* **2021**, 8984-8990.
42. Lowell, J.; Rose-Innes, A. C., Contact electrification. *Advances in Physics* **1980,** 29, (6), 947-1023.
43. Liu, J.; Jiang, K.; Lan, N.; Li, Z.; Thundat, T., Interfacial friction-induced electronic excitation mechanism for tribo-tunneling current generation. *Materials Horizons* **2019**, 6, 1020-1026.
44. Diaz, A. F.; Wollmann, D.; Dreblow, D., Contact electrification: ion transfer to metals and polymers. *Chemistry of Materials* **1991,** 3, 997-999.
45. McCarty, L. S.; Whitesides, G. M., Electrostatic charging due to separation of ions at interfaces: contact electrification of ionic electrets. *Angewandte Chemie International Edition* **2008,** 47, (12), 2188-207.
46. Baytekin, H. T.; Baytekin, B.; Soh, S.; Grzybowski, B. A., Is water necessary for contact electrification? *Angewandte Chemie International Edition* **2011,** 50, (30), 6766-70.
47. Apodaca, M. M.; Wesson, P. J.; Bishop, K. J.; Ratner, M. A.; Grzybowski, B. A., Contact electrification

between identical materials. *Angewandte Chemie International Edition* **2010,** 49, (5), 946-9.
48. Baytekin, H. T.; Patashinski, A. Z.; Branicki, M.; Baytekin, B.; Soh, S.; Grzybowski, B. A., The Mosaic of Surface Charge in Contact Electrification. *Science* **2011,** 333, (6040), 308-312.
49. Baytekin, H. T.; Baytekin, B.; Incorvati, J. T.; Grzybowski, B. A., Material transfer and polarity reversal in contact charging. *Angewandte Chemie International Edition* **2012,** 51, (20), 4843-7.
50. Li, S.; Zhou, Y.; Zi, Y.; Zhang, G.; Wang, Z. L., Excluding Contact Electrification in Surface Potential Measurement Using Kelvin Probe Force Microscopy. *ACS Nano* **2016,** 10, (2), 2528-35.
51. Willatzen, M.; Lin Wang, Z., Theory of contact electrification: Optical transitions in two-level systems. *Nano Energy* **2018,** 52, 517-523.
52. Pan, S.; Zhang, Z., Triboelectric effect: A new perspective on electron transfer process. *Journal of Applied Physics* **2017,** 122, (14), 144302.
53. Lin, S.; Xu, L.; Xu, C.; Chen, X.; Wang, A. C.; Zhang, B.; Lin, P.; Yang, Y.; Zhao, H.; Wang, Z. L., Electron Transfer in Nanoscale Contact Electrification: Effect of Temperature in the Metal-Dielectric Case. *Advanced Materials* **2019,** 31, (17), e1808197.
54. Xu, C.; Zhang, B.; Wang, A. C.; Zou, H.; Liu, G.; Ding, W.; Wu, C.; Ma, M.; Feng, P.; Lin, Z.; Wang, Z. L., Contact-Electrification between Two Identical Materials: Curvature Effect. *ACS Nano* **2019,** 13, (2), 2034-2041.
55. Wang, Z. L.; Wang, A. C., On the origin of contact-electrification. *Materials Today* **2019,** 30, 34-51.
56. Zou, H.; Zhang, Y.; Guo, L.; Wang, P.; He, X.; Dai, G.; Zheng, H.; Chen, C.; Wang, A. C.; Xu, C.; Wang, Z. L., Quantifying the triboelectric series. *Nature Communications* **2019,** 10, (1), 1427.
57. Zhang, X.; Chen, L.; Jiang, Y.; Lim, W.; Soh, S., Rationalizing the Triboelectric Series of Polymers. *Chemistry of Materials* **2019,** 31, (5), 1473-1478.
58. Pandey, R. K.; Sun, Y.; Nakanishi, H.; Soh, S., Reversible and Continuously Tunable Control of Charge of Close Surfaces. *J Phys Chem Lett* **2017,** 8, (24), 6142-6147.
59. Pandey, R. K.; Ao, C. K.; Lim, W.; Sun, Y.; Di, X.; Nakanishi, H.; Soh, S., The Relationship between Static Charge and Shape. *ACS Central Science* **2020,** 6, (5), 704-714.
60. Salaneck, W. R.; Paton, A.; Clark, D. T., Double mass transfer during polymer-polymer contacts. *Journal of Applied Physics* **1976,** 47, (1), 144-147.
61. Šutka, A.; Mālnieks, K.; Lapčinskis, L.; Kaufelde, P.; Linarts, A.; Bērziņa, A.; Zābels, R.; Jurķāns, V.; Gorņevs, I.; Blūms, J.; Knite, M., The role of intermolecular forces in contact electrification on polymer surfaces and triboelectric nanogenerators. *Energy & Environmental Science* **2019,** 12, (8), 2417-2421.
62. Lapčinskis, L.; Mālnieks, K.; Blūms, J.; Knite, M.; Oras, S.; Käämbre, T.; Vlassov, S.; Antsov, M.; Timusk, M.; Šutka, A., The Adhesion-Enhanced Contact Electrification and Efficiency of Triboelectric Nanogenerators. *Macromolecular Materials and Engineering* **2020,** 305, (1), 1900638.
63. Baytekin, H. T.; Baytekin, B.; Incorvati, J. T.; Grzybowski, B. A., Material transfer and polarity reversal in contact charging. *Angewandte Chemie International Edition* **2012,** 51, (20), 4843-4847.
64. Baytekin, H.; Patashinski, A.; Branicki, M.; Baytekin, B.; Soh, S.; Grzybowski, B. A., The mosaic of surface charge in contact electrification. *Science* **2011,** 333, (6040), 308-312.
65. Zhang, J.; Rogers, F. J. M.; Darwish, N.; Goncales, V. R.; Vogel, Y. B.; Wang, F.; Gooding, J. J.; Peiris, M. C. R.; Jia, G.; Veder, J. P.; Coote, M. L.; Ciampi, S., Electrochemistry on Tribocharged Polymers Is Governed by the Stability of Surface Charges Rather than Charging Magnitude. *Journal of the American Chemical Society* **2019,** 141, (14), 5863-5870.
66. Sakaguchi, M.; Makino, M.; Ohura, T.; Iwata, T., Contact electrification of polymers due to electron transfer among mechano anions, mechano cations and mechano radicals. *Journal of Electrostatics* **2014,** 72, (5), 412-416.
67. Yun, C.; Lee, S. H.; Ryu, J.; Park, K.; Jang, J. W.; Kwak, J.; Hwang, S., Can Static Electricity on a Conductor Drive a Redox Reaction: Contact Electrification of Au by Polydimethylsiloxane, Charge Inversion in Water, and Redox Reaction. *Journal of the American Chemical Society* **2018,** 140, (44), 14687-14695.
68. Xia, X.; Wang, H.; Guo, H.; Xu, C.; Zi, Y., On the material-dependent charge transfer mechanism of the contact electrification. *Nano Energy* **2020,** 78.
69. Nie, J.; Ren, Z.; Xu, L.; Lin, S.; Zhan, F.; Chen, X.; Wang, Z. L., Probing Contact-Electrification-Induced Electron and Ion Transfers at a Liquid-Solid Interface. *Advanced Materials* **2020,** 32, (2), e1905696.
70. Lin, Z. H.; Cheng, G.; Lin, L.; Lee, S.; Wang, Z. L., Water-solid surface contact electrification and its use for harvesting liquid-wave energy. *Angewandte Chemie International Edition* **2013,** 52, (48), 12545-9.
71. Lin, S.; Xu, L.; Chi Wang, A.; Wang, Z. L., Quantifying electron-transfer in liquid-solid contact electrification and the formation of electric double-layer. *Nature Communications* **2020,** 11, (1), 399.
72. Xu, C.; Zi, Y.; Wang, A. C.; Zou, H.; Dai, Y.; He, X.; Wang, P.; Wang, Y.-C.; Feng, P.; Li, D.; Wang, Z. L., On the Electron-Transfer Mechanism in the Contact-Electrification Effect. *Advanced Materials* **2018,** 30, (15), 1706790.
73. Maeda, N.; Chen, N.; Tirrell, M.; Israelachvili, J. N., Adhesion and Friction Mechanisms of Polymer-on-Polymer Surfaces. *Science* **2002,** 297, (5580), 379-382.

74. Fan, F.-R.; Tian, Z.-Q.; Lin Wang, Z., Flexible triboelectric generator. *Nano Energy* **2012,** 1, (2), 328-334.
75. Tcho, I.-W.; Kim, W.-G.; Jeon, S.-B.; Park, S.-J.; Lee, B. J.; Bae, H.-K.; Kim, D.; Choi, Y.-K., Surface structural analysis of a friction layer for a triboelectric nanogenerator. *Nano Energy* **2017,** 42, 34-42.
76. Ke, K. H.; Chung, C. K., High-Performance Al/PDMS TENG with Novel Complex Morphology of Two-Height Microneedles Array for High-Sensitivity Force-Sensor and Self-Powered Application. *Small* **2020,** 16, (35), e2001209.
77. Cheng, G.-G.; Jiang, S.-Y.; Li, K.; Zhang, Z.-Q.; Wang, Y.; Yuan, N.-Y.; Ding, J.-N.; Zhang, W., Effect of argon plasma treatment on the output performance of triboelectric nanogenerator. *Applied Surface Science* **2017,** 412, 350-356.
78. Zhang, X.-W.; Li, G.-Z.; Wang, G.-G.; Tian, J.-L.; Liu, Y.-L.; Ye, D.-M.; Liu, Z.; Zhang, H.-Y.; Han, J.-C., High-Performance Triboelectric Nanogenerator with Double-Surface Shape-Complementary Microstructures Prepared by Using Simple Sandpaper Templates. *ACS Sustainable Chemistry & Engineering* **2018,** 6, (2), 2283-2291.
79. Sun, J.-G.; Yang, T. N.; Kuo, I. S.; Wu, J.-M.; Wang, C.-Y.; Chen, L.-J., A leaf-molded transparent triboelectric nanogenerator for smart multifunctional applications. *Nano Energy* **2017,** 32, 180-186.
80. Trinh, V. L.; Chung, C. K., A Facile Method and Novel Mechanism Using Microneedle-Structured PDMS for Triboelectric Generator Applications. *Small* **2017,** 13, (29).
81. Huang, J.; Fu, X.; Liu, G.; Xu, S.; Li, X.; Zhang, C.; Jiang, L., Micro/nano-structures-enhanced triboelectric nanogenerators by femtosecond laser direct writing. *Nano Energy* **2019,** 62, 638-644.
82. Nguyen, V.; Zhu, R.; Yang, R., Environmental effects on nanogenerators. *Nano Energy* **2015,** 14, 49-61.
83. Lee, K. Y.; Chun, J.; Lee, J. H.; Kim, K. N.; Kang, N. R.; Kim, J. Y.; Kim, M. H.; Shin, K. S.; Gupta, M. K.; Baik, J. M.; Kim, S. W., Hydrophobic sponge structure-based triboelectric nanogenerator. *Advanced Materials* **2014,** 26, (29), 5037-42.
84. Baytekin, H. T.; Baytekin, B.; Grzybowski, B. A., Mechanoradicals created in "polymeric sponges" drive reactions in aqueous media. *Angewandte Chemie International Edition* **2012,** 51, (15), 3596-600.
85. Zhou, Q.; Lee, K.; Kim, K. N.; Park, J. G.; Pan, J.; Bae, J.; Baik, J. M.; Kim, T., High humidity- and contamination-resistant triboelectric nanogenerator with superhydrophobic interface. *Nano Energy* **2019,** 57, 903-910.
86. Yang, Y.; Jing, T.; Xu, B., Self-Assembly of Porous Microstructured Polydimethylsiloxane Films for Wearable Triboelectric Nanogenerators. *Macromolecular Materials and Engineering* **2020**. 202000276
87. Tang, Y.; Zheng, Q.; Chen, B.; Ma, Z.; Gong, S., A new class of flexible nanogenerators consisting of porous aerogel films driven by mechanoradicals. *Nano Energy* **2017,** 38, 401-411.
88. Lee, C.; Yang, S.; Choi, D.; Kim, W.; Kim, J.; Hong, J., Chemically surface-engineered polydimethylsiloxane layer via plasma treatment for advancing textile-based triboelectric nanogenerators. *Nano Energy* **2019,** 57, 353-362.
89. Liu, L.; Yang, X.; Zhao, L.; Xu, W.; Wang, J.; Yang, Q.; Tang, Q., Nanowrinkle-patterned flexible woven triboelectric nanogenerator toward self-powered wearable electronics. *Nano Energy* **2020,** 73.
90. Zhou, Q.; Kim, J.-N.; Han, K.-W.; Oh, S.-W.; Umrao, S.; Chae, E. J.; Oh, I.-K., Integrated dielectric-electrode layer for triboelectric nanogenerator based on Cu nanowire-Mesh hybrid electrode. *Nano Energy* **2019,** 59, 120-128.
91. Wu, J.; Wang, X.; Li, H.; Wang, F.; Yang, W.; Hu, Y., Insights into the mechanism of metal-polymer contact electrification for triboelectric nanogenerator via first-principles investigations. *Nano Energy* **2018,** 48, 607-616.
92. Yu, N.; Polycarpou, A. A., Adhesive contact based on the Lennard–Jones potential: a correction to the value of the equilibrium distance as used in the potential. *Journal of Colloid and Interface Science* **2004,** 278, (2), 428-435.
93. Myshkin, N.; Kovalev, A., Adhesion and surface forces in polymer tribology—A review. *Friction* **2018,** 6, (2), 143-155.
94. Lin, S.; Xu, L.; Zhu, L.; Chen, X.; Wang, Z. L., Electron Transfer in Nanoscale Contact Electrification: Photon Excitation Effect. *Advanced Materials* **2019,** 31, (27), e1901418.
95. Xu, C.; Zi, Y.; Wang, A. C.; Zou, H.; Dai, Y.; He, X.; Wang, P.; Wang, Y. C.; Feng, P.; Li, D.; Wang, Z. L., On the Electron-Transfer Mechanism in the Contact-Electrification Effect. *Advanced Materials* **2018,** 30, (15), e1706790.
96. Li, S.; Zhou, Y.; Zi, Y.; Zhang, G.; Wang, Z. L., Excluding contact electrification in surface potential measurement using kelvin probe force microscopy. *ACS nano* **2016,** 10, (2), 2528-2535.
97. Zhou, Y. S.; Liu, Y.; Zhu, G.; Lin, Z.-H.; Pan, C.; Jing, Q.; Wang, Z. L., In Situ Quantitative Study of Nanoscale Triboelectrification and Patterning. *Nano Letters* **2013,** 13, (6), 2771-2776.
98. Lin, S.; Xu, L.; Xu, C.; Chen, X.; Wang, A. C.; Zhang, B.; Lin, P.; Yang, Y.; Zhao, H.; Wang, Z. L., Electron Transfer in Nanoscale Contact Electrification: Effect of Temperature in the Metal–Dielectric Case. *Advanced Materials* **2019,** 31, (17), 1808197.
99. Lin, S.; Xu, L.; Zhu, L.; Chen, X.; Wang, Z. L., Electron Transfer in Nanoscale Contact Electrification:

Photon Excitation Effect. *Advanced Materials* **2019,** 31, (27), 1901418.
100. Chung, C. K.; Ke, K. H., High contact surface area enhanced Al/PDMS triboelectric nanogenerator using novel overlapped microneedle arrays and its application to lighting and self-powered devices. *Applied Surface Science* **2020,** 508.
101. Chen, A.; Zhang, C.; Zhu, G.; Wang, Z. L., Polymer Materials for High-Performance Triboelectric Nanogenerators. *Advanced Science* **2020,** 7, (14), 2000186.
102. Choi, Y. S.; Kim, S.-W.; Kar-Narayan, S., Materials-Related Strategies for Highly Efficient Triboelectric Energy Generators. *Advanced Energy Materials* **2021,** 11, (7), 2003802.
103. Dharmasena, R. D. I. G., Inherent asymmetry of the current output in a triboelectric nanogenerator. *Nano Energy* **2020,** 76.
104. Šutka, A.; Sherrell, P. C.; Shepelin, N. A.; Lapčinskis, L.; Mālnieks, K.; Ellis, A. V., Measuring Piezoelectric Output—Fact or Friction? *Advanced Materials* **2020,** 32, (32), 2002979.
105. Askari, H.; Khajepour, A.; Khamesee, M. B.; Saadatnia, Z.; Wang, Z. L., Piezoelectric and triboelectric nanogenerators: Trends and impacts. *Nano Today* **2018,** 22, 10-13.
106. Ahmed, A.; Hassan, I.; Helal, A. S.; Sencadas, V.; Radhi, A.; Jeong, C. K.; El-Kady, M. F., Triboelectric Nanogenerator versus Piezoelectric Generator at Low Frequency (<4 Hz): A Quantitative Comparison. *iScience* **2020,** 23, (7), 101286.
107. Ryu, H.; Yoon, H.-J.; Kim, S.-W., Hybrid Energy Harvesters: Toward Sustainable Energy Harvesting. *Advanced Materials* **2019,** 31, (34), 1802898.
108. Jiang, D.; Su, Y.; Wang, K.; Wang, Y.; Xu, M.; Dong, M.; Chen, G., A triboelectric and pyroelectric hybrid energy harvester for recovering energy from low-grade waste fluids. *Nano Energy* **2020,** 70, 104459.
109. Pang, Y.; Cao, Y.; Derakhshani, M.; Fang, Y.; Wang, Z. L.; Cao, C., Hybrid Energy-Harvesting Systems Based on Triboelectric Nanogenerators. *Matter* **2021,** 4, (1), 116-143.
110. Marvan, M.; Havránek, A. In *Flexoelectric effect in elastomers*, Darmstadt, 1988; Steinkopff: Darmstadt, 1988; pp 33-36.
111. Mizzi, C. A.; Lin, A. Y. W.; Marks, L. D., Does Flexoelectricity Drive Triboelectricity? *Physical Review Letters* **2019,** 123, (11), 116103.
112. Zhang, M.; Yan, D.; Wang, J.; Shao, L.-H., Ultrahigh flexoelectric effect of 3D interconnected porous polymers: modelling and verification. *Journal of the Mechanics and Physics of Solids* **2021,** 151, 104396.
113. Šutka, A.; Mālnieks, K.; Lapčinskis, L.; Timusk, M.; Kalniņš, K.; Kovaļovs, A.; Bitenieks, J.; Knite, M.; Stevens, D.; Grunlan, J., Contact electrification between identical polymers as the basis for triboelectric/flexoelectric materials. *Physical Chemistry Chemical Physics* **2020,** 22, (23), 13299-13305.
114. Persson, B. N. J., On the role of flexoelectricity in triboelectricity for randomly rough surfaces. *EPL (Europhysics Letters)* **2020,** 129, (1), 10006.

AUTHOR INFORMATION

Corresponding Author

* Dr Peter C. Sherrell (peter.sherrell@unimelb.edu.au); Prof. Amanda V. Ellis (amanda.ellis@unimelb.edu.au)

Author Contributions

The manuscript was written through contributions of all authors. All authors have given approval to the final version of the manuscript.

Funding Sources

The authors would like to acknowledge the funding from the Australian Research Council Linkage Program (LP160100071).

ACKNOWLEDGMENT

The authors would like to acknowledge the funding from the Australian Research Council Linkage Program (LP160100071).

Table of Contents Graphic